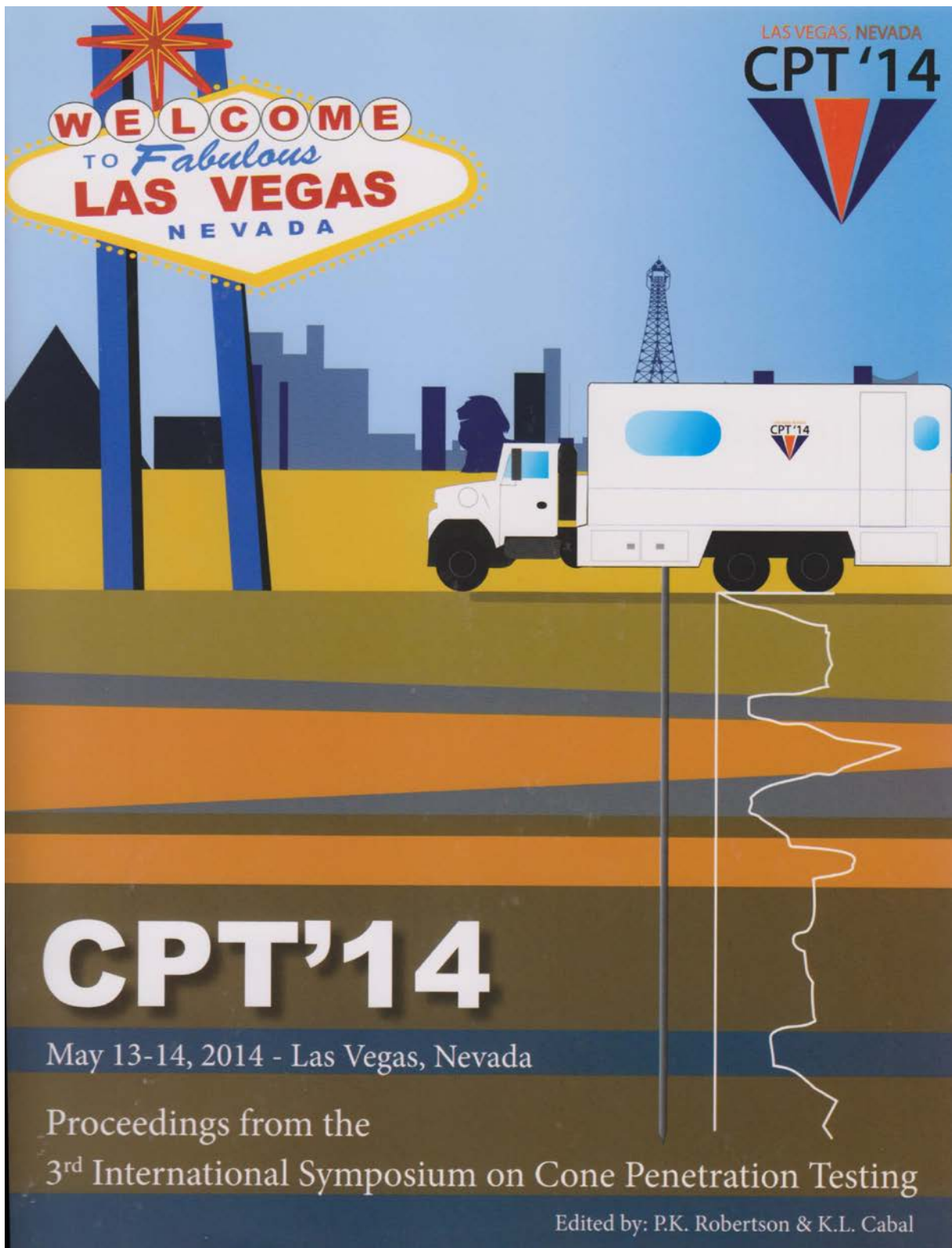Mayne, P.W. (2014). KN2: Interpretation of geotechnical parameters from seismic piezocone tests. *Proceedings, 3rd International Symposium on Cone Penetration Testing* (CPT'14, Las Vegas), ISSMGE Technical Committee TC 102, Edited by P.K. Robertson and K.I. Cabal: p 47-73.   www.cpt14.com

WELCOME TO *Fabulous* LAS VEGAS NEVADA

LAS VEGAS, NEVADA
CPT'14

CPT'14

May 13-14, 2014 - Las Vegas, Nevada

Proceedings from the
3rd International Symposium on Cone Penetration Testing

Edited by: P.K. Robertson & K.L. Cabal

Interpretation of geotechnical parameters from seismic piezocone tests

P.W. Mayne
Georgia Institute of Technology, Atlanta, GA USA

ABSTRACT: Soil behavior is complex and thus requires quantification by a reasonably good number of different engineering parameters. Consequently, the seismic piezocone test (SCPTu) is particularly well-suited to being an efficient and economical tool for routine site characterization because four independent readings are obtained with depth by a single sounding: q_t, f_s, u_2, and V_s. An overview on using all four of these separate measurements for evaluating soil engineering parameters is given, realizing in some cases that redundancy occurs when two or more readings are used to interpret the same geomaterial parameter. The assessment of parameters and subsurface information herein includes: unit weight, soil type, relative density of sands, effective stress peak friction angle, undrained shear strength, effective yield stress, and stiffness.

1 INTRODUCTION

1.1 *Cone and piezocone penetration test (CPTu)*

During normal CPT advancement at 20 mm/s, near continuous vertical readings of cone tip resistance (q_t), sleeve friction (f_s), and penetration porewater pressure (u_2) are obtained at 1- to 5-cm depth intervals to profile the geostratigraphy and determine local soil conditions at that location. These three measurements may further be used either separately or together to evaluate soil engineering parameters, including state of stress, strength, and stiffness.

During a halt in penetration that often occurs at the 1-m rod breaks, readings of excess porewater pressure decay with time can also be recorded. The results are useful in establishing the hydrostatic conditions, as well as possible artesian groundwater conditions or drawdown. The time to reach 50% consolidation provides a benchmark dissipation reading (t_{50}) that can be evaluated to give the coefficient of consolidation and/or soil permeability.

1.2 *Seismic piezocone penetration test (SCPTu)*

Horizontally-oriented geophones within the penetrometer can be employed to measure the arrival times from surface-generated shear waves and provide the magnitude of downhole shear wave velocity (V_s). The resultant hybrid testing contains geotechnical, hydrological, and geophysical data, termed the seismic piezocone test (SCPTu), and offers an expedient and efficient means to collect a wealth of geotechnical information with depth from a single sounding: q_t, f_s, u_2, and V_s (Campanella, et al. 1986).

A representative SCPTu from the eastern suburbs of New Orleans is presented in Figure 1 with four recorded channels shown versus depth next to an interpreted soil profile. The complex stratigraphy at this site is evident and substantiates the importance of site investigative practices that offer near continuous resistance measurements so that small thin layers are not missed.
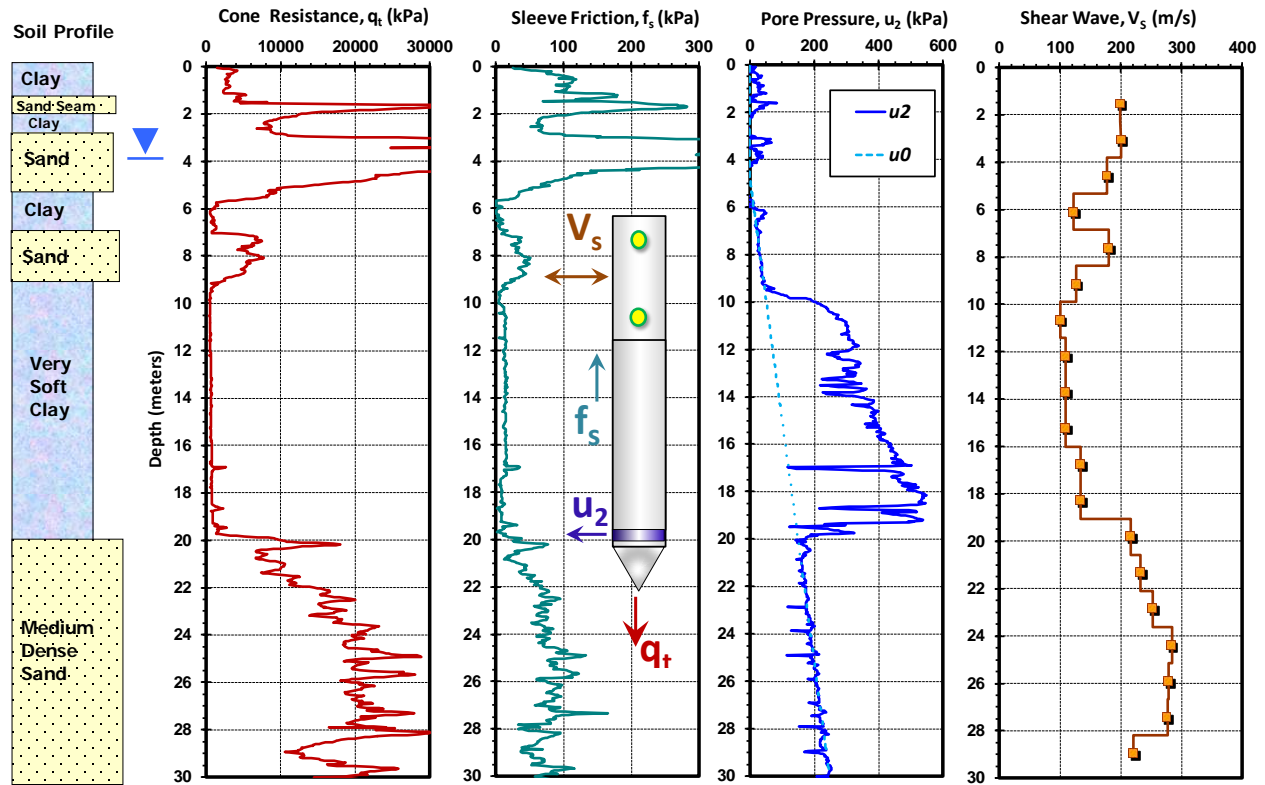
Figure 1. Representative seismic piezocone sounding from New Orleans East Levees

The measured readings from the SCPTu can be interpreted using a variety of theoretical, analytical, and statistical methods towards establishing a suite of geotechnical engineering parameters that are needed in the analysis and design of construction projects. Soil parameters are many and may include: unit weight, soil type, relative density, friction angle, dilatancy angle, preconsolidation stress, undrained shear strength, lateral stress coefficient, elastic modulus, permeability, and other variables. In certain relationships, a single measurement may provide an estimate of a particular soil parameter, while in other cases, two or more readings may be required. Moreover, with multiple methods available, it is possible to have corroborating evaluations from two different approaches, yet also plausible to find conflicting estimates where two approaches do not agree. In the latter case, perhaps this represents the situation of a "red flag" or warning that additional testing (laboratory tests on undisturbed samples; or alternate in-situ pressuremeter or flat dilatometer tests) is warranted to resolve the issue.

2 SOIL UNIT WEIGHT

2.1 General case: all soil types

In the case of SCPTu where shear wave velocities are available, a global relationship for total soil unit weight was found from a large database derived from a variety of noncemented soils (Mayne 2007a):

$$\gamma_t \, (kN/m^3) \; = \; 8.32 \log (V_s) \; - \; 1.61 \log (z) \tag{1}$$

where V_s (m/s) and depth z (m).

   When only CPTu data are obtained, a trend has been identified between the total unit weight, sleeve friction, and effective stress (Mayne and Peuchen 2012). A direct unit weight relationship with the
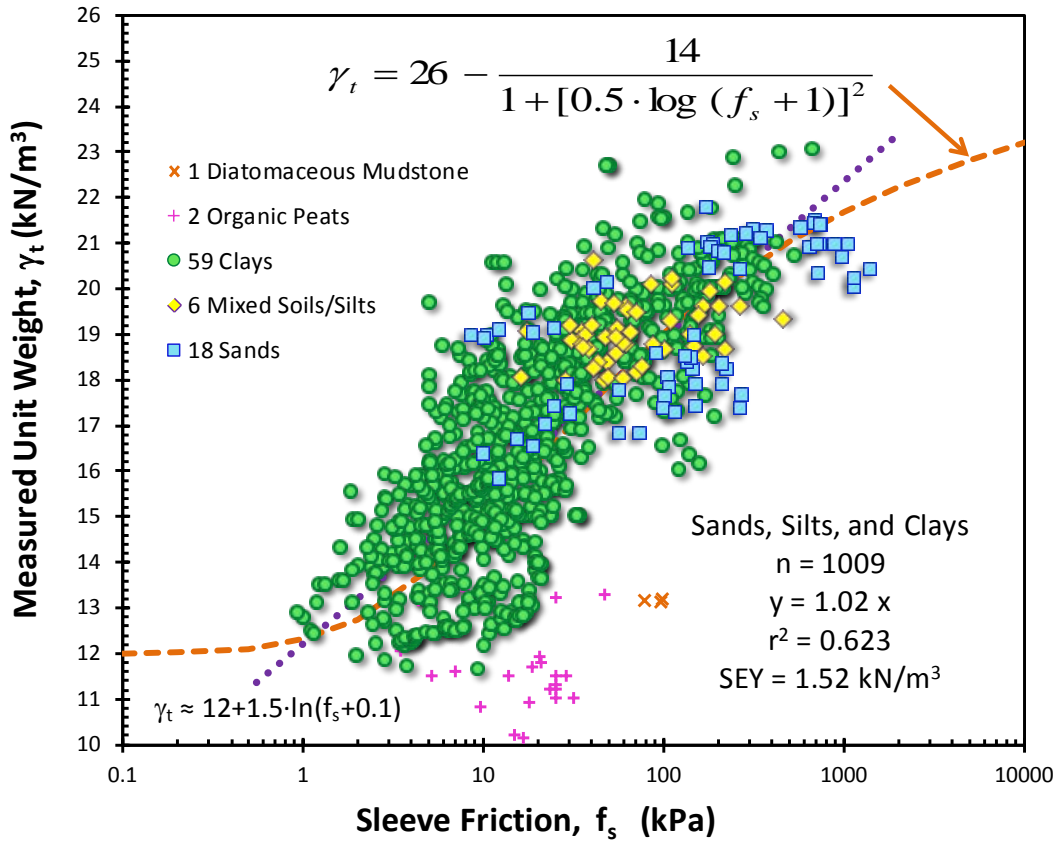
Figure 2. Global trend of total soil unit weight with sleeve friction reading in various soils

sleeve friction is also observed, as presented in Figure 2:

$$\gamma_t = 26 - \frac{14}{1+[0.5 \cdot \log(f_s +1)]^2} \qquad (2a)$$

where the specific units include: γ_t (kN/m^3) and f_s (kPa). Alternatively, a simpler expression is:

$$\gamma_t \approx 12 + 1.5 \ln(f_s + 1) \qquad (2b)$$

While it is well known that the sleeve friction is perhaps the weakest in reliability of the three piezocone readings, in such a relationship the unit weight is increasing by a factor of two (11.5 kN/m^3 $\leq \gamma_t \leq$ 23 kN/m^3) while the sleeve friction is spanning three orders of magnitude (1 kPa $\leq$ f$_s$ $\leq$ 1000 kPa), thus an accurate f$_s$ is not necessary given that the expected variance is on the order of $\pm$ 1.5 kN/m^3 in the estimated value of unit weight. Also, as would be implied by consideration of (1) and (2) together, a direct trend between V$_s$ and f$_s$ might be likely, as presented elsewhere (Mayne 2007b). Of added note, an independent method for estimating gt from CPT is given by Robertson & Cabal (2010).

2.2 Soft to firm normally-consolidated clays

In the case of recent Holocene clays that exhibit normally-consolidated to lightly-overconsolidated states of stress, a parameter termed the cone resistance-depth ratio ($m_q = \Delta q_t/\Delta z$) can be defined directly from the measured CPT plots. For NC to LOC clays, the best-fit line (intercept = 0) is essentially identical with the linear regression line from least squares fitting (i.e., $m_q = \Delta q_t/\Delta z \approx q_t/z$). A quick estimate of the total soil unit weight for the deposit is then found from (Mayne and Peuchen 2012):

$$\gamma_t = \gamma_w + m_q/8 \qquad (3)$$

where γ_w = unit weight of water. The γ_t vs. m_q trend is presented in Figure 3. Of added interest is that m_q, γ_t, and γ_w are all in the same units (i.e., kN/m³).

An example set of CPTu data recently acquired (Miller, 2012) at the Canadian national test site in South Gloucester, Ontario (McRostie and Crawford 2001) is presented in Figure 4a illustrating the determination of the slope parameter $m_q = (\Delta q_t/\Delta z) = 42.8$ kN/m³. Using equation (3) gives an estimated γ_t = 15.4 kN/m³ for the clay that compares quite well with measured unit weights at the site, specifically the mean value $\gamma_t = 15.8$ kN/m³ from tube samples.

Further statistical analyses of the database in soft NC to LOC clays showed that soil unit weights may vary locally with depth, so that a means to capture some local variations could be found from (Mayne and Peuchen 2012):

$$\gamma_t = 0.636\,(q_t)^{0.072}\,(10 + m_q/8) \tag{4}$$

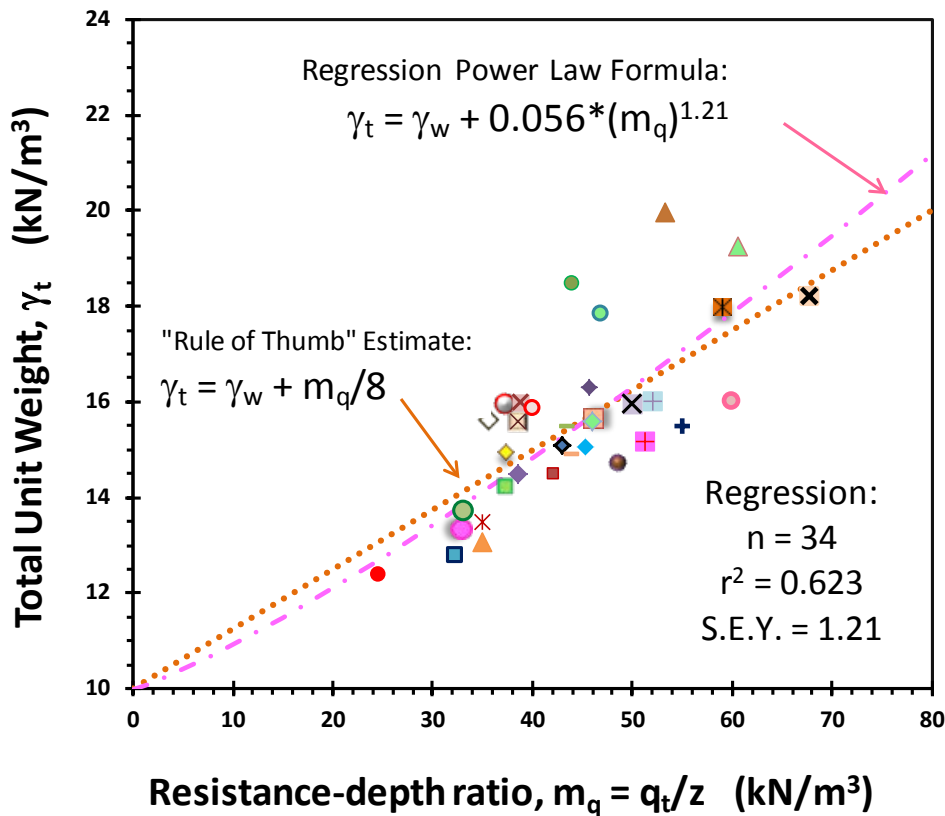where the units-dependent values of m_q and γ_t are in kN/m³ and q_t is in kPa.

Figure 3. Relationship between unit weight of soft-firm NC-LOC clays and resistance-depth ratio (m_q)

2.3 *Stiff to hard clays*

When the parameter $m_q > 80$, the slope of the Δq_t-Δz trend will not pass through the origin and a comparison of the best-fit (intercept = 0) and least squares regression lines will show deviations from each other (i.e., intercept ≠ 0). As a consequence, soil unit weight ceases to increase further with the apparent slope $m_q = q_t/z$. Figure 4 shows these observations with the higher apparent m_q values grouping into three categories: (a) stiff to hard intact clays, (b) fissured clays, and (c) carbonate fine-grained soils.
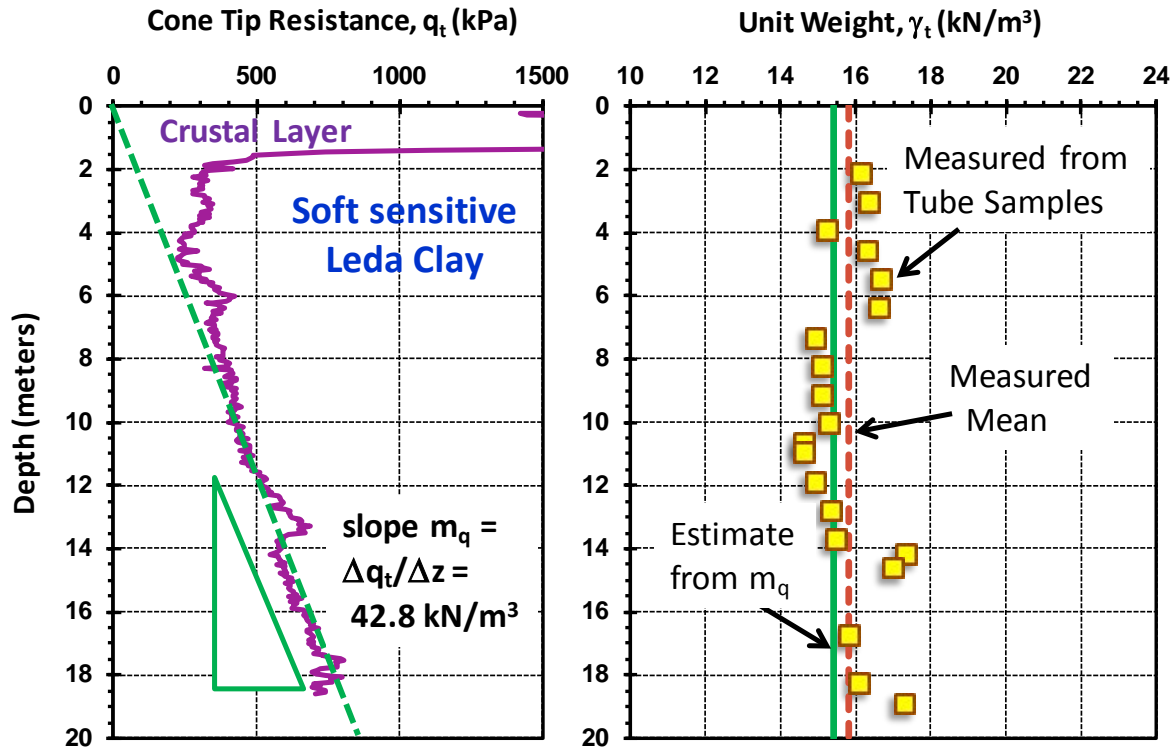
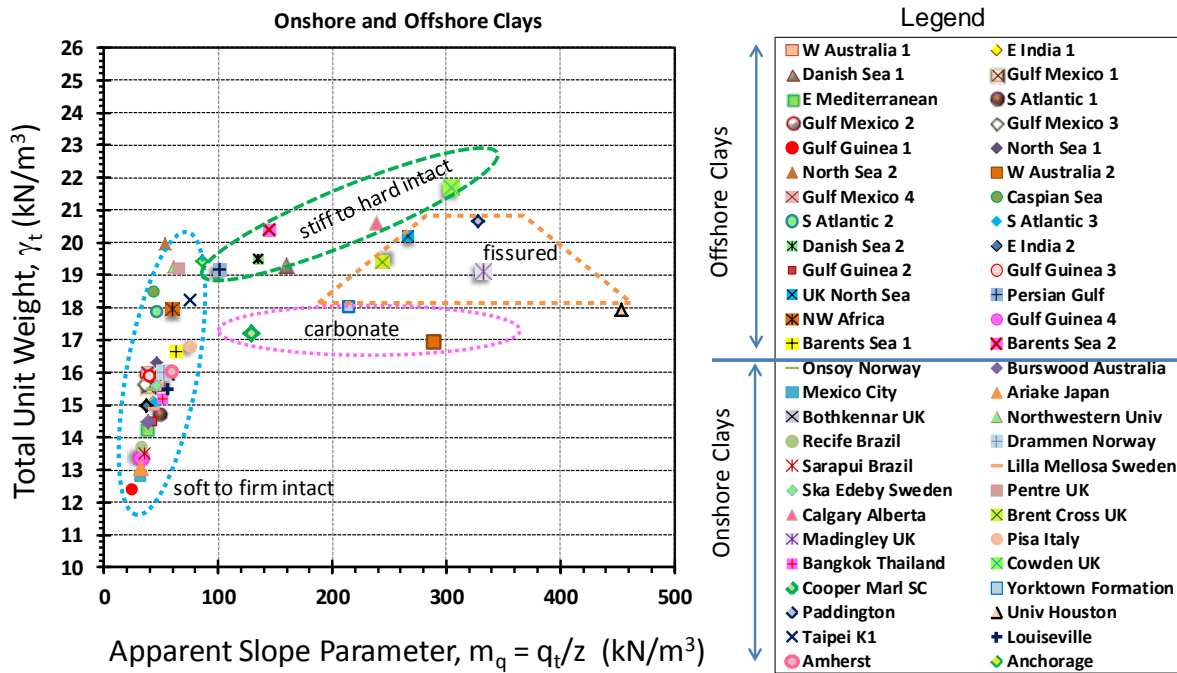Figure 4. Profiles from South Gloucester test site: (a) cone resistance and (b) unit weight with depth

Figure 5. General trends between unit weight of soft-firm-stiff-hard clays and resistance-depth ratio (m_q) indicating regions of hard intact soils, fissured clays, and calcareous geomaterials.

3   SOIL BEHAVIORAL TYPE

Soil classification via CPT and CPTu is indirect and can be handled by one or more of three general approaches: (1) rules of thumb (Mayne et al. 2002), (2) soil behavioral charts (Robertson 2009), and (3) probabilistic methods (Tumay et al. 2008). Any of the methods should be cross-checked and verified for a particular geologic setting before routine use in practice.

   The development of a CPT material index (I_c) has been found advantageous in the initial screening of soil types and helps to organize the sounding into 9 different zones of similar soil response. In this case, the CPT index is found from (Robertson 2009):

$$I_c = \sqrt{(3.47 - \log Q_{tn})^2 + (1.22 + \log F_r)^2} \tag{5}$$

where Q_{tn} = stress-normalized cone tip resistance and F_r = normalized sleeve friction, as detailed in Figure 6. The material index groups the soil layers into zones 2 through 7, allowing a quick identification of soil type. Sensitive soils of zone 1 can be screened by employing the following expression:

Zone 1: $Q_{tn} < 12 \exp(-1.4 \cdot F_r)$ $\tag{6}$

The stiff soils of zone 8 ($1.5\% < F_r < 4.5\%$) and zone 9 ($F_r > 4.5\%$) can be identified from:

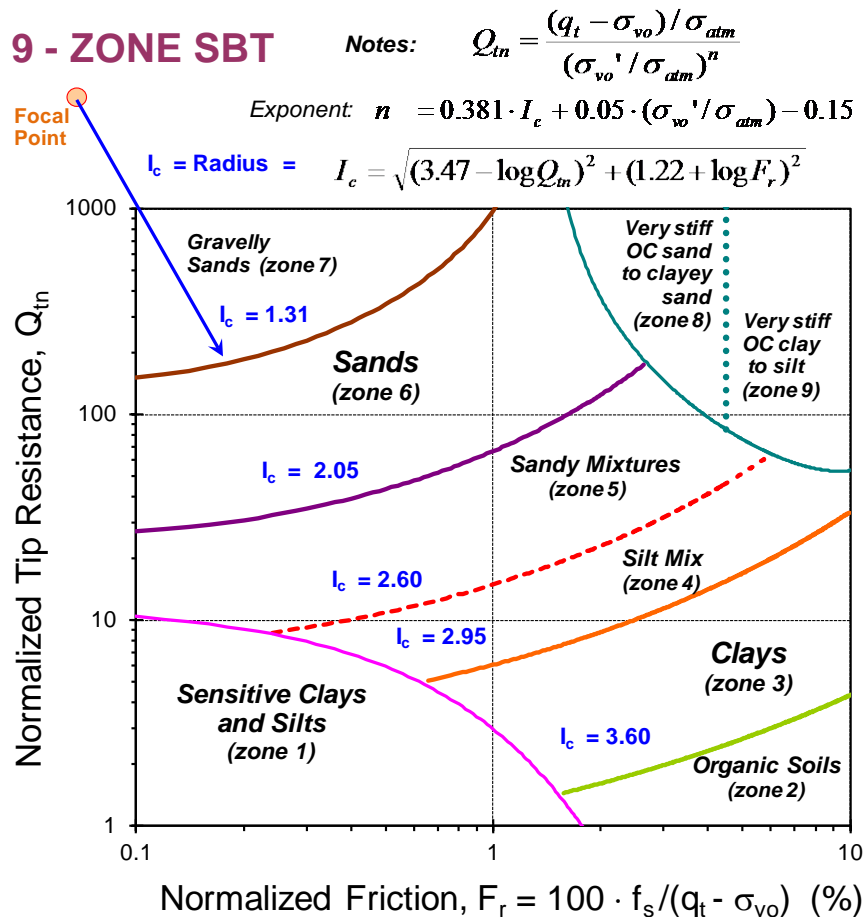Zones 8 and 9: $Q_{tn} > \dfrac{1}{0.005(F_r - 1) - 0.0003(F_r - 1)^2 - 0.002}$ $\tag{7}$

Figure 6.   Soil behavioral type from Q_{tn}-F_r chart with nine zonal classification (after Robertson 2009)
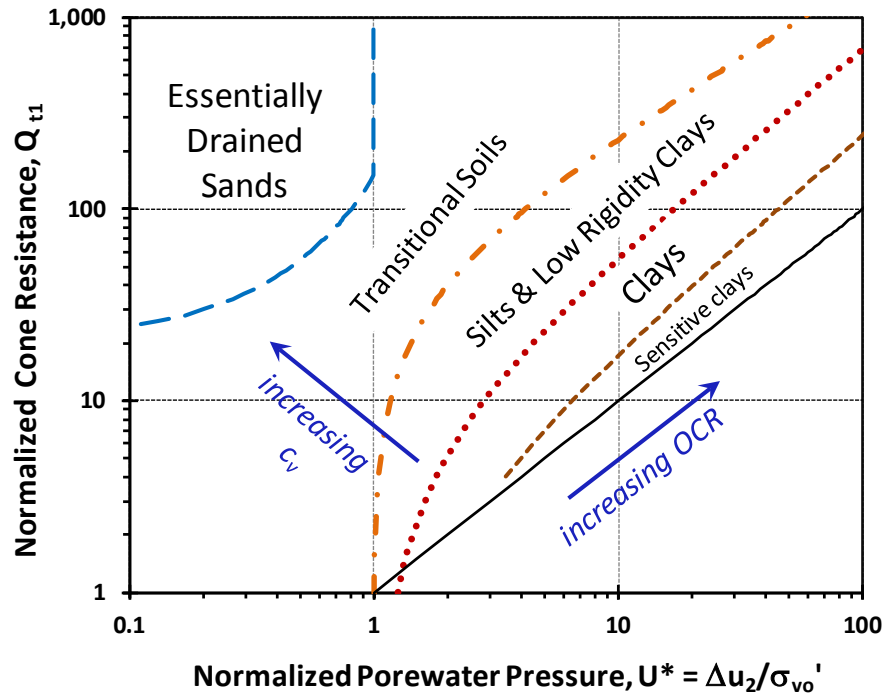
Figure 7. CPT indirect classification for soil behavioral type from Q_{t1}-$\Delta u_2/\sigma_{vo}'$ chart (Schneider et al. 2008)

After zones 1, 8, and 9 are first detected, the material index I_c can subsequently be used in a set of nested if-then statements within a spreadsheet to assign zones 2 through 7 accordingly.

The interpretation of soil behavior often relies upon a total stress analysis that forces the assumption of either a fully-drained condition characteristic of clean sands, otherwise an undrained response attributed to clays. The condition of drained loading refers specifically to the case where no excess porewater pressures ($\Delta u = 0$) are induced above the hydrostatic value (u_0), whereas undrained loading corresponds to conditions of constant volume ($\Delta V/V_0 = 0$). Robertson (2009) has suggested that drained response essentially occurs when $I_c < 2.5$ while undrained behavior dominates when $I_c > 2.7$.

Of course, the measured porewater pressures can be accommodated into the CPT classification scheme to further delineate the type of soil response. For the shoulder reading of pressure (u_2), Robertson (1990) used the normalized parameter $B_q = (u_2-u_0)/(q_t-\sigma_{vo})$ while Eslami and Fellenius (1997) incorporated these into an effective cone resistance: $q_E = q_t - u_2$. More recently, Schneider et al. (2008) used the normalized cone resistance: $Q_{t1} = (q_t-\sigma_{vo})/\sigma_{vo}'$ vs. the porewater pressure parameter $U^* = \Delta u_2/\sigma_{vo}'$ to form soil behavioral regions by analytical considerations of undrained, partially-drained, to fully-drained response of the soil, as presented in Figure 7. This approach helps to better identify intermediate soil types, such as zones 1, 4, and 5 in the SBT chart as indicated in Figure 6.

Recent efforts by Robertson (2012) have unified the CPT soil classifications from older non-normalized SBT charts that use q_t and friction ratio (FR) with the newer 9-part SBT charts that use Q_{tn} and F_r. In addition, categories of contractive and dilative soil behavior can be recognized.

4 COMPACTNESS OF SANDS

4.1 *Relative density of quartz-silica sands*

The degree of compactness of clean sands has long been expressed in terms of relative density (D_R), although in more recent efforts, the state parameter (Ψ_s) has found interest because of its application to critical state soil mechanics and a rational framework towards understanding of soil liquefaction problems (Jefferies and Been 2006; Robertson 2009, 2010).

For the classical problem of evaluating D_R from CPTs in quartz and silica sands, Jamiolkowski et al. (2001) reviewed calibration chamber test data that were corrected for boundary size effects (i.e., D/d ratio, where D = chamber diameter and d = cone diameter) with additional considerations regarding the relative compressibility of the sands. Supplemented with the few data available on undisturbed sand samples (Mayne 2006), Figure 8 presents their derived relationship for relative density in terms of stress-normalized cone tip resistance that can be expressed:

$$D_R(\%) = 100 \cdot \left[0.268 \cdot \ln(q_{t1}) - b_x \right] \qquad (8)$$

where $q_{t1} = (q_t/\sigma_{atm})/(\sigma_{vo}'/\sigma_{atm})^{0.5}$ is a stress-normalized cone resistance rather similar in magnitude to Q_{tn} (Robertson 2009). The term $b_x = 0.675$ as found from regression analyses on normally-consolidated (NC) clean sands. Jamiolkowski et al. (2001) show three lines corresponding to different sand compressibilities: high ($b_x = 0.525$), medium ($b_x = 0.675$), and low ($b_x = 0.825$). Their guidance suggests that sands of high compressibility include mica sands, calcareous sands, and carbonate sands. Siliceous sands (approximately equal parts of quartz and feldspar) comprise the medium compressibility range. Sands of low compressibility include those of quartz, such as Ottawa sand.

Note that sleeve friction readings were not generally available from the chamber test series to allow determination of Q_{tn} which has a variable exponent n dependent upon the material index I_c. Thus, q_{t1} has been used herein for Q_{tn} in clean sands.
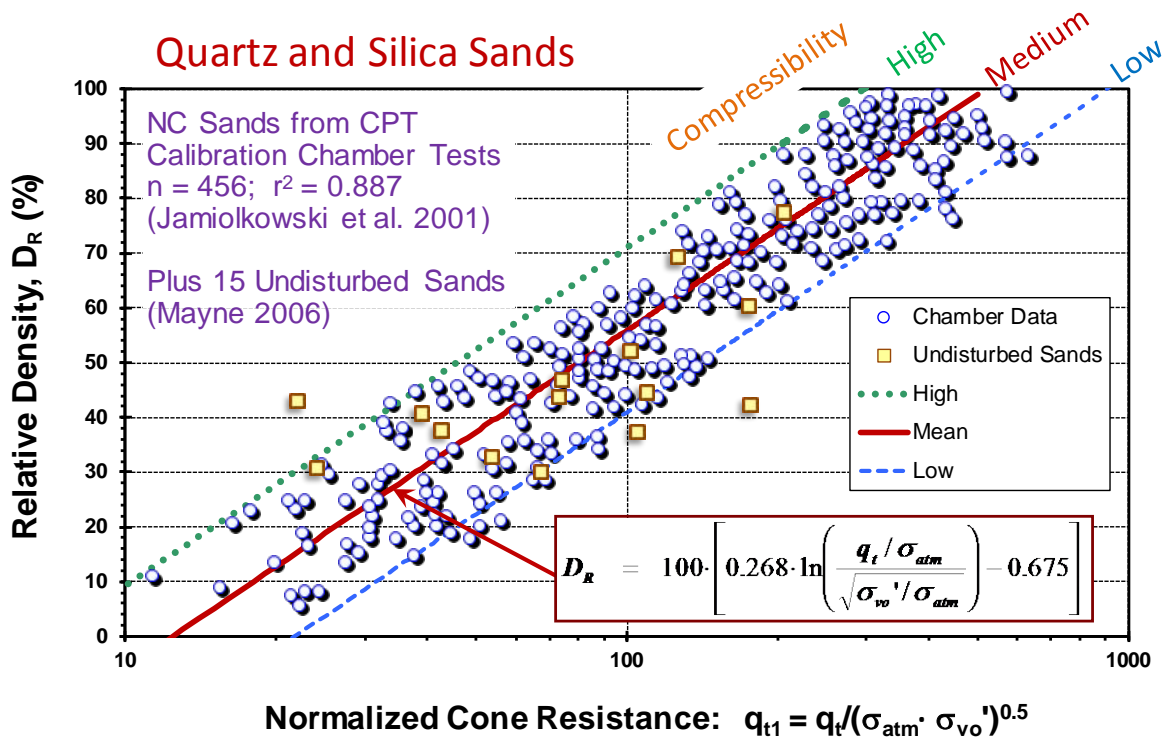

Figure 8. Relative density evaluation from CPTs on NC quartz to silica sands (Jamiolkowski et al. 2001)

From chamber test data on eight preconsolidated sands, the effects of overconsolidation for the mean trend may be approximated by (Mayne 2009):

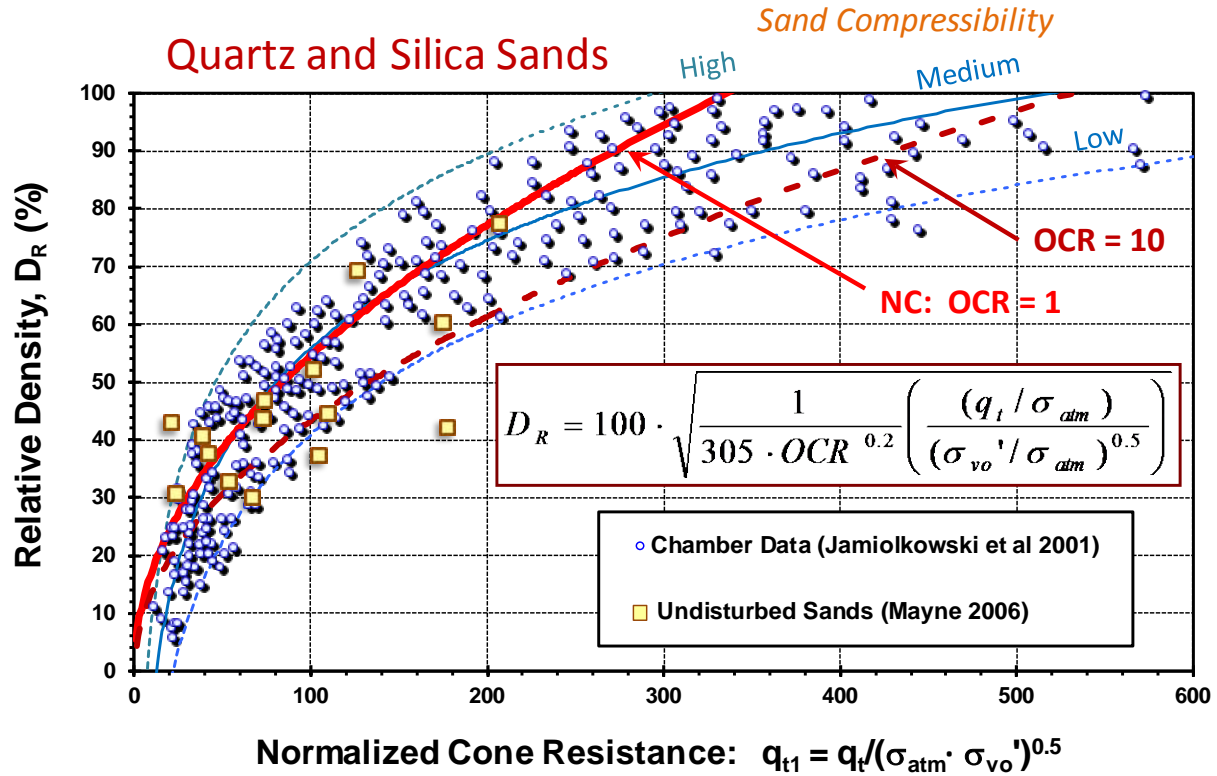$$b_x \approx 0.675 \cdot OCR^{0.2} \qquad (9)$$

Figure 9. Relative density trends from CPT chamber tests on NC and OC quartz to silica sands

A separate evaluation of the D_R relationship with cone tip resistances in sands was made by Kulhawy & Mayne (1990) who adopted the format recommended by Skempton (1986) in his studies of D_R with SPT resistances. For the statistical mean trends involving mainly quartz-silica type sands, an account of the effects of stress history was quantified, expressed by:

$$D_R \, (\%) \quad = \quad 100 \sqrt{\frac{q_{t1}}{305 \cdot OCR^{0.2}}} \tag{10}$$

A re-examination of the data in arithmetic plots, Figure 9 shows that equations (9) and (10) provide very comparable values of D_R from normalized cone tip resistances for NC sands over much of the range of relative densities, parting ways slightly when D_R exceeds 80%.

4.2 Relative density of calcareous-carbonate sands

Calibration chamber tests have also been used with prepared deposits of calcareous-carbonate sands. Table 1 provides a summary of index parameters on 6 carbonate sands that were tested in CPT chambers, including: Quiou (Fioravante et al. 1998); Dogs Bay (Nutt and Houlsby 1991), Ewa (Morioka and Nicholson 2000), Kingfish (Parkin 1991), Kenya (Jamiolkowski et al 2001), and Jeju (Kim et al. 2009; Lee et al. 2010).

Interestingly, the trend of D_R with normalized q_{t1} for carbonate sands is not logarithmic nor square-root based, but appears to be linear. In an alternative plotting scheme, Figure 10 presents the trend of q_{t1} vs. D_R from the available six series of chamber tests on carbonate sands. When $D_R < 30\%$, the measured cone tip resistances are about equal for all data sets, suggesting that loose sands behave somewhat com-

parably during full-displacement type penetration despite their mineralogical differences. However, for $D_R > 30\%$, the trends for quartz-silica sands show significant increases in cone resistance, since the hard particles must be forced aside during penetration. On the other hand, the trends for calcareous-carbonate sands remain similar when $D_R > 30\%$ implying grain breakage, fracturing, and crushing as the particles are pushed closer together as they approach their minimum packing arrangement (i.e., e_{min}). The trends for carbonate sands appear to be rather independent of calcite content in the range $42\% < CaCO_3 < 98\%$ and indicate simply that:

$$D_R \, (\%) \;\; = \;\; 0.87 \, q_{t1} \tag{11}$$

Also presented here are the two prior (mean) relationships for quartzitic and silicaceous sands. Consideration can be given to using these plots as a plausible means to boost the q_{t1} readings of carbonate sands to equivalent values representative of quartz-silica types sands. In that case, the trends in Figure 11 (average based on the Kulhawy-Mayne 1990 and Jamiolkowski et al 2001 relationships for quartzitic and silicaceous sands), the following correction factor may be suggested:

$$CF \;\; = \;\; \frac{q_{t1}(silica-quartz)}{q_{t1}(calcareous-carbonate)} \;\; = \;\; 6 - \frac{5}{1+(D_R/100)^4} \tag{12}$$

This function is a modified hyperbola that gives a correction factor of 1 for the range: $0 < D_R \le 30\%$ and then when $D_R > 30\%$, *CR* increases with relative density up to a maximum of value 3.5 when $D_R = 100\%$. A correction or "shell factor" has been found useful on ground modification projects when carbonate sands are present and results need to be equalized for specification controls (Kirsh & Kirsch 2010). For instance, a shell factor developed for vibrocompaction operations in Dubai sands at the large Isles of Palm project found (Wehr 2006):

$$CF \;\; = \;\; f_{shell} \;\; = \;\; 1.36 \; + \; 0.0046 \, D_R \tag{13}$$

This is seen to be a more modest trend with relative density than the aforementioned expression.

Table 1. List of 6 carbonate sands tested in CPT calibration chamber series

| Sand Name =	Quiou	Dogs Bay	Ewa	Kingfish	Kenya	Jeju	NOTES and
Location =	France	Ireland	Hawaii	Australia	Africa	S. Korea	REMARKS
D_{50} mm=	0.58	0.25	0.80	0.30	0.13	0.41	= Mean Grain Size (mm)
PF % =	3.00	0.10	1.00	7.00	0	1.00	= Percent Fines (< 0.075 mm)
UC =	4.52	2.66	5.60	3.05	1.86	1.61	= D_{60}/D_{10} = Uniformity Coefficient
G_s =	2.72	2.75	2.70	2.71	2.785	2.79	= specific gravity of solids
e_{max} =	1.28	1.83	1.30	1.53	1.778	1.44	= maximum void ratio
e_{min} =	0.83	0.98	0.66	1.07	1.283	1.03	= minimum void ratio
$CaCO_3$ (%) =	77	87 to 92%	98	"high"	97	42.60	= percent calcium carbonate content
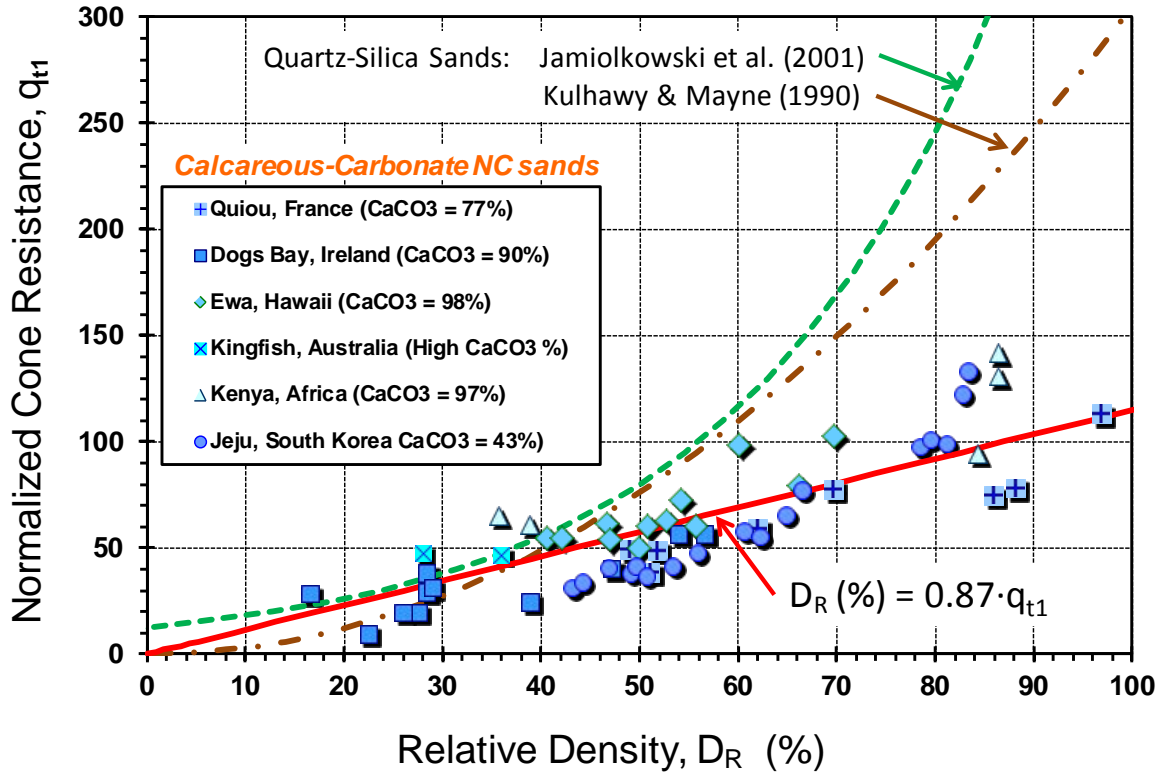
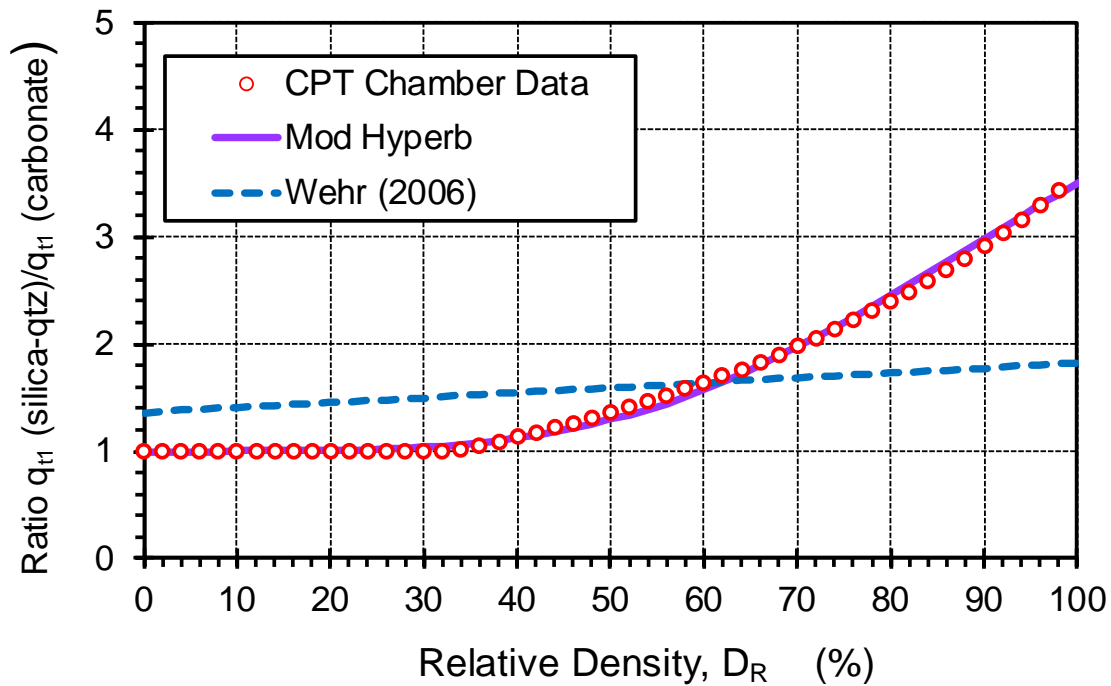Figure 10. Normalized cone resistance versus relative density from CPT chamber data on NC carbonate sands

Figure 11. Correction factor for converting q_{t1} of calcareous sands to equivalent q_{t1} values of silica sands.
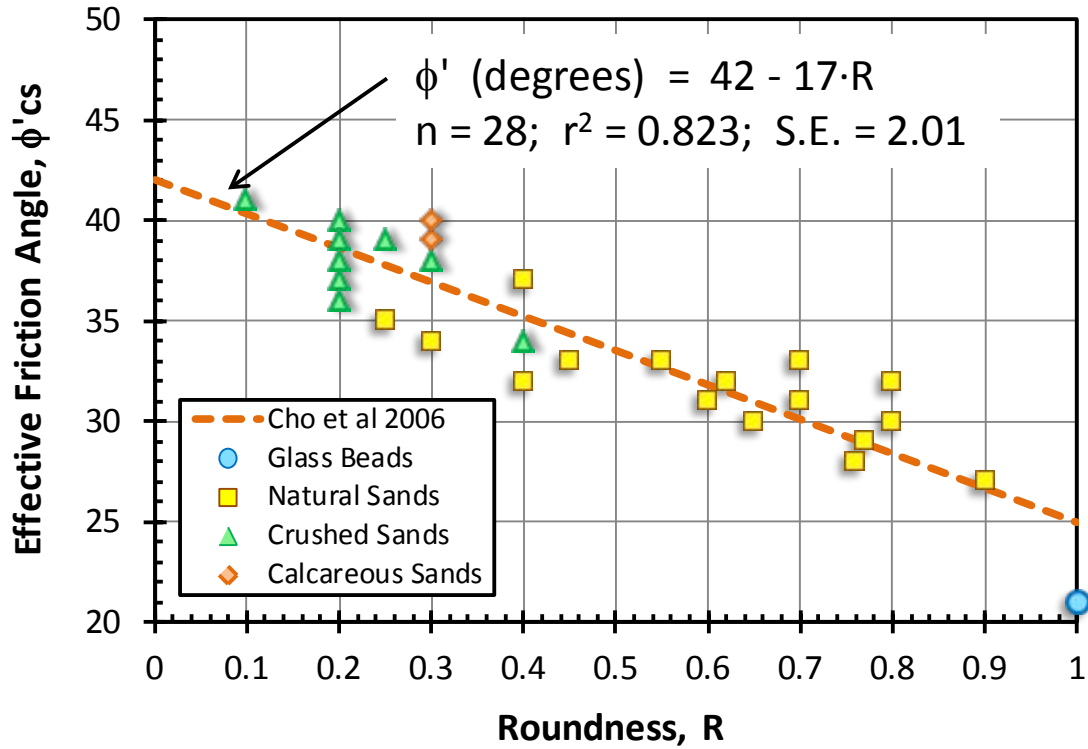
Figure 12. Trend of base friction angle (ϕ_{cs}') with particle roundness (R) reported by Cho et al. (2006). Note: for very rounded sands, R = 1; very angular sands, R = 0.

5 EFFECTIVE FRICTION ANGLE

5.1 *Friction angle of sands*

The drained (effective stress) friction angle (ϕ') of soils is a fundamental property that controls much of its behavioral response to loading and initial stress state. In terms of the commonly-adopted Mohr-Coulomb strength criterion, the shear strength (or maximum shear stress, τ_{max}) is expressed:

$$\tau_{max} = c' + \sigma_n' \tan\phi' \tag{14}$$

where c' = effective cohesion intercept (generally: c' = 0 for unbonded geomaterials). In many cases, the normal stress can be taken equal to the effective vertical stress: $\sigma_n' = \sigma_{vo}'$.

The peak friction angle (ϕ_p') of sands is composed of two components: (1) a basic frictional value (designated ϕ_{cs}' for critical state) that is due to particle grain shape, compressibility characteristics, and mineralogy; and (2) a dilatancy effect (quantified by ψ_d, the dilatancy angle) which reflects the relative packing of particles (e_0 or D_R or Ψ_s) and ambient stress level, expressed in terms of either mean effective stress, $p' = \frac{1}{3}(\sigma_v' + 2\sigma_h')$ or more practically, in terms of the effective vertical stress (σ_v'), albeit their magnitudes might be required at failure states rather than the initial conditions. Together, the two components combine to produce a peak friction angle:

$$\phi_p' \approx \phi_{cs}' + \psi_d' \tag{15}$$

Characteristic values of ϕ_{cs}' are on the order of 32° for quartz sands, 33° for silty quartz sands with up to 20% fines content, 34° for siliceous sands (quartz-feldspar), 39° for calcareous sands, and 40° for feldspathic sands (Bolton 1986; Salgado et al. 2000; Jamiolkowski et al. 2001). The friction angle also depends upon mode of testing (i.e., plane strain vs. triaxial) and direction of loading (compression vs. extension). For the triaxial compression mode, Cho et al. (2006) showed a clear trend of ϕ_{cs}' in terms of particle roundness (R) for a wide range of natural and crushed sands of varied mineralogy (Figure 12), which indicated:

$$\phi_{cs}' \ = \ 42° \ - \ 17 \, R \tag{16}$$

For assessing peak friction angle (ϕ_p') of sands from CPT, there are several approaches: (a) use of a dilatancy framework where q_{t1} provides the input value of D_R (Bolton, 1986); (b) inverse bearing capacity from cavity expansion or limit plasticity theories (Yu & Mitchell, 1998; Schnaid 2009); (c) numerical simulation by finite elements or discrete elements (e.g., Salgado et al. 1998); (d) estimating the dilatancy angle (ψ_d') from CPT relationships (Tokimatsu et al. 1995), (e) state parameter relationships (Jefferies and Been 2006), or (f) direct CPT methods (Lunne et al. 1997; Mayne 2006). Towards a validation exercise, an elite database was compiled from special expensive undisturbed (frozen) samples of clean sands that were tested under triaxial compression modes to derive ϕ_p' values. A total of 17 sand sites were subjected to in-situ SPT, CPT, and V_s measurements, as well as other lab and field tests (summarized by Mayne 2006, 2009).

The triaxial data from undisturbed sands fit nicely with the expression derived by Kulhawy & Mayne (1990) that was developed on the basis of CPT calibration chamber data (primarily quartz-silica sands) which had been corrected for boundary size effects:

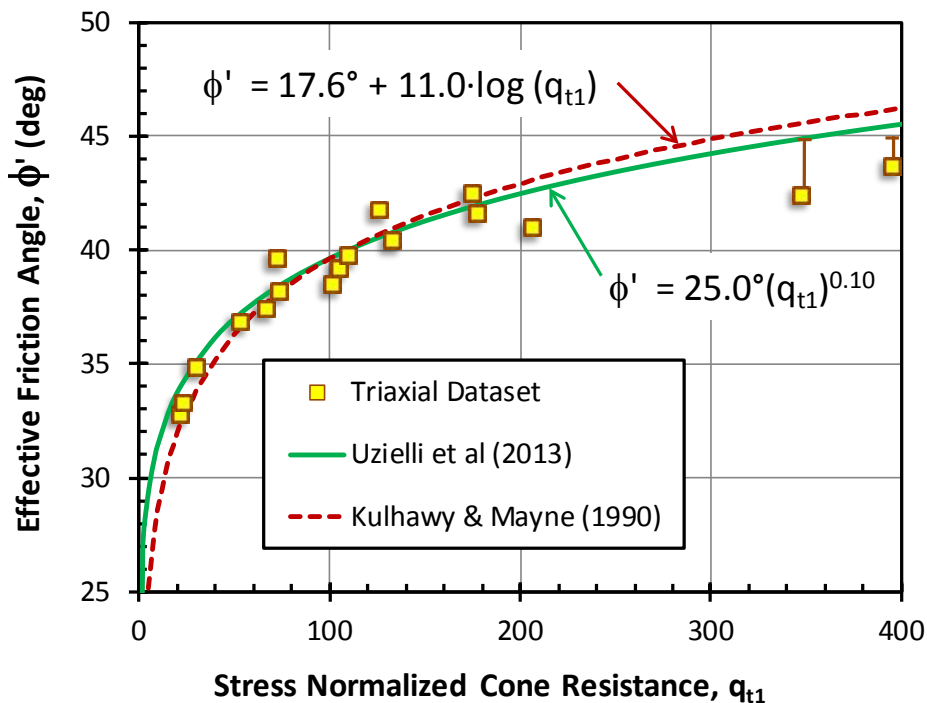$$\phi_p' \ (\text{degrees}) \ = \ 17.6° + 11.0 \log (q_{t1}) \tag{17}$$

Figure 13. Direct relationships between peak friction angle of quartz-silica sands and normalized cone resistance

A re-evaluation of these data in terms of reliability and probabilistic considerations was made by Uzielli et al (2013) using a power law form to obtain the deterministic expression:

$$\phi_p' \text{ (degrees) } = 25.0° \, (q_{t1})^{0.10} \tag{18}$$

which gave very similar results to the aforementioned log function (see Figure 13). Here, the intent was to assign design values of ϕ_p' so that a target probability (p_t) of non-exceedance occurs. The results are shown in Figure 14 for several levels of p_t = 0.10, 0.05, 0.01, and 0.005. The relationships shown primarily apply to clean quartz to siliceous sands having trace to little fines content (FC < 10%).

For SCPTu soundings, an additional assessment of ϕ_p' is afforded from the shear wave velocity data. Following the probabilistic study by Uzielli et al. (2013), an analogous trend was developed:

$$\phi_p' \text{ (degrees) } = 3.9° \, (V_{S1})^{0.44} \tag{19}$$

where $V_{S1} = V_S/(\sigma_{vo}'/\sigma_{atm})^{0.25}$ = stress-normalized shear wave velocity (m/s) and the relationships for different probabilities of nonexceedance are presented in Figure 15.

For sands of high calcareous content, methodologies to obtain ϕ_p' are provided by Jamiolkowski et al. (2001) and Robertson (2010). From a research needs standpoint, undisturbed (frozen) sampling and triaxial testing of calcareous and carbonate sands, as well as silica-carbonates, would be welcomed.
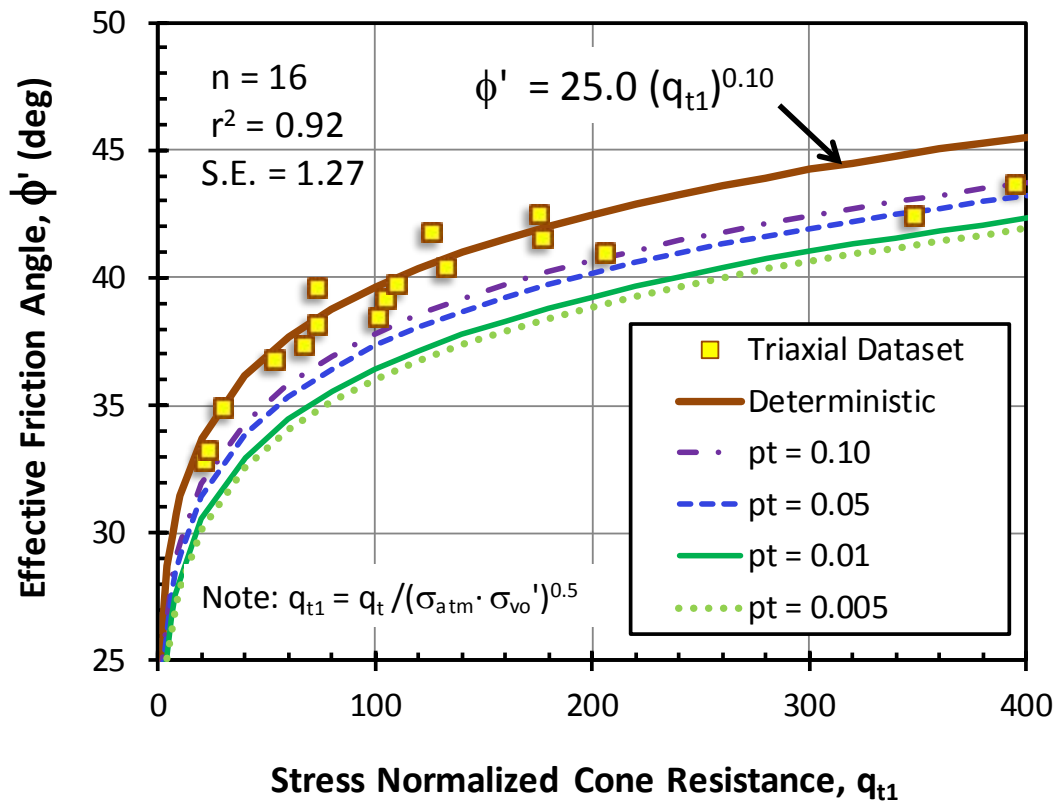

Figure 14. Probability curves between peak friction angle of quartz-silica sands and normalized cone resistance
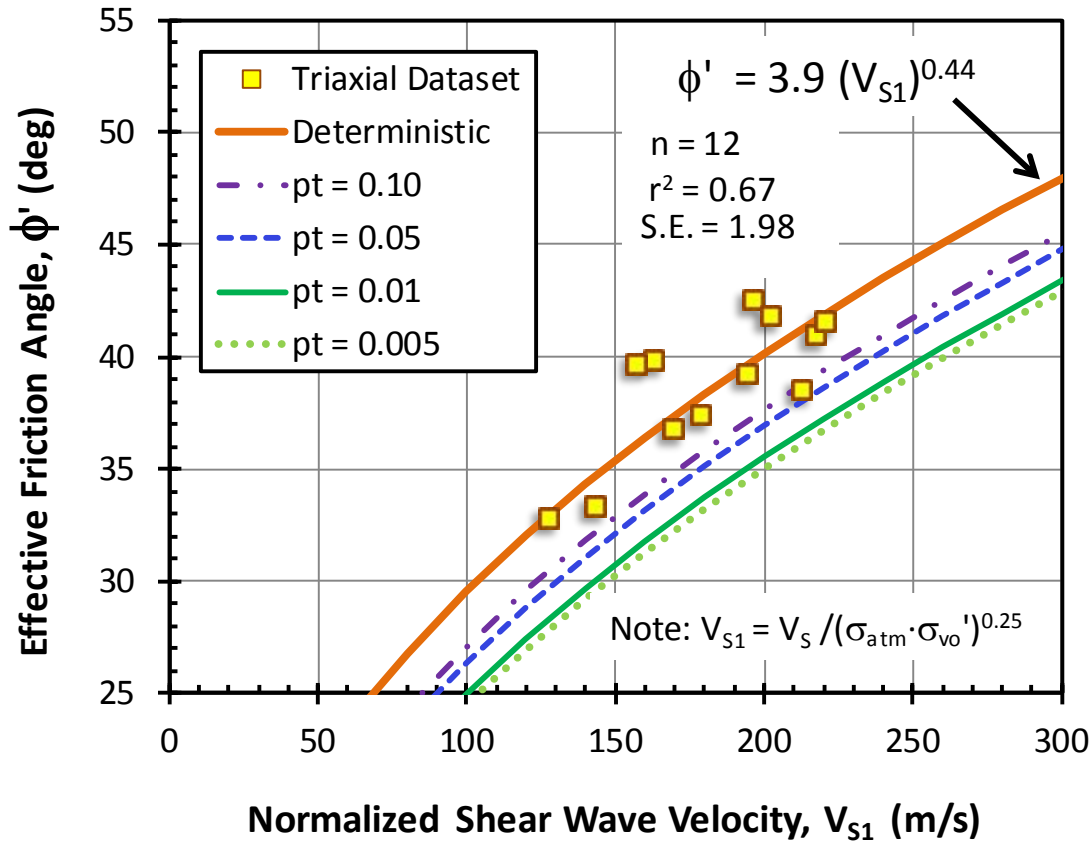
Figure 15. Probability curves between peak friction angle of quartz-silica sands and normalized shear wave

5.2 *Effective Friction Angle of Clays and Silts*

For silts and clays which exhibit excess porewater pressures during penetration ($B_q > 0.1$), an effective stress limit plasticity solution for undrained penetration can be implemented towards the evaluation of ϕ' (Sandven & Watn 1995). In this approach, the cone resistance number (N_m) is defined by:

$$N_m = \frac{N_q - 1}{1 + N_u \cdot B_q} = \frac{q_t - \sigma_{v0}}{\sigma_{vo}' + a'} \qquad (20)$$

where $a' = c' \cdot \cot\phi'$ = effective attraction, $N_q = K_p \cdot \exp[(\pi-2\beta) \cdot \tan\phi']$ = tip bearing capacity factor, $K_p = (1+\sin\phi')/(1-\sin\phi')$ is the passive lateral stress coefficient, β = angle of plastification ($-40° < \beta < +30°$) that defines the size of the failure zone around the tip, and $N_u = 6 \cdot \tan\phi' \cdot (1+\tan\phi')$ = porewater pressure bearing factor. The full solution allows for an interpretation of a paired set of effective stress Mohr-Coulomb strength parameters (c' and ϕ') for all soil types: sands, silts, and clays, as well as mixed soils. For the case where $\beta = 0$ (Terzaghi equation), the relationship for ϕ' in terms of N_m and B_q is presented in graphical form (Figure 16). Also, note that when $c' = a' = 0$, the parameter $N_m = Q_{t1}$.
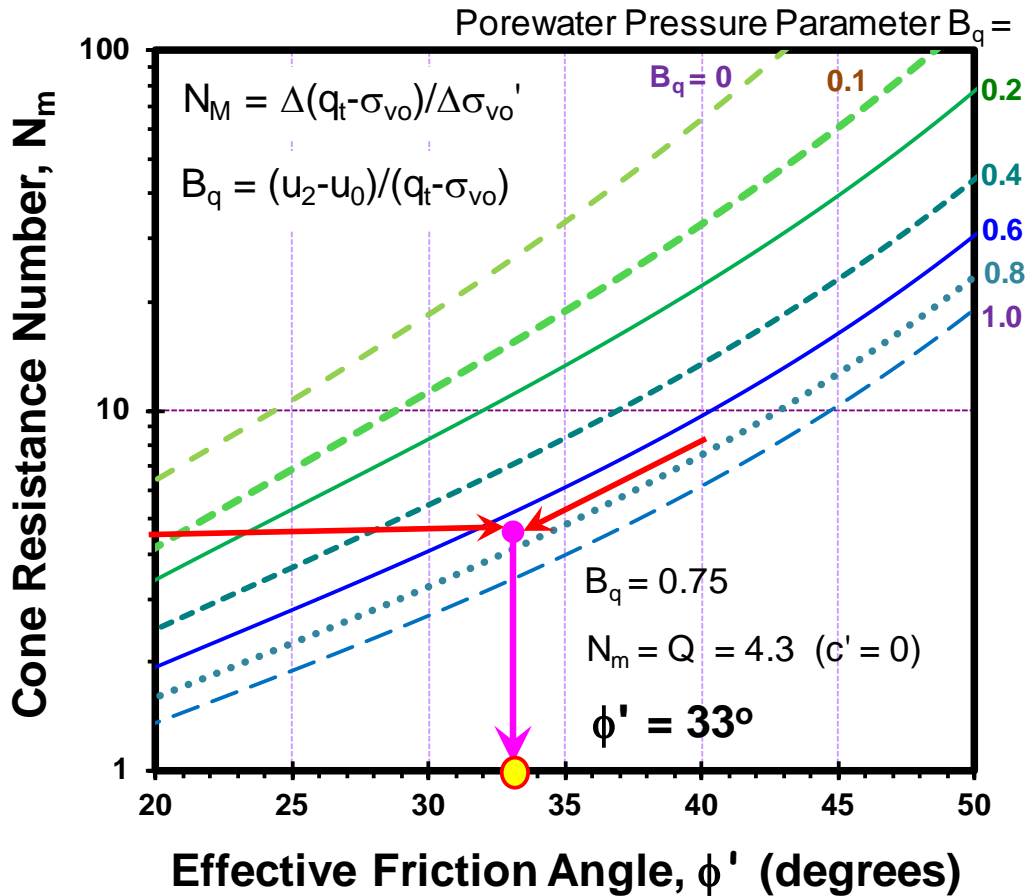
Figure 16. NTH Method for evaluating ϕ' from CPTu in silts and clays (modified after Sanven & Watn 1995)
Note: specific values cited are for case study of CPTu from northwestern Idaho

5.3 Case Study: Sandpoint Idaho

   To illustrate the use of the NTH method, results from an 80-m deep CPTu conducted for the Idaho DOT State Route 95 bridge and embankments in Sandpoint, Idaho are used (Figure 17). Primarily, the sounding penetrates through a soft to firm clayey silt deposit with a few sand layers evident in the upper 10 m, from 50 to 53 m, and 60 to 66 m. Numerous sand "stringers" and lenses can be seen at other depths. For the post-processing, we are interested in the fine grained clayey silts, thus have chosen some representative points along various elevations in the profile, as indicated by the open square dots.
   The procedure for determining the cone resistance number (N_m) is found as the slope from plotting net cone tip resistance vs. the effective overburden stress, as illustrated in Figure 18a. In this instance, we force the line through the origin (assuming $c' = 0$) to obtain $N_m = Q = 4.2$. Note that if allowed, a negative intercept on the abscissa axis would be the value of the attraction (a') that would give the effective cohesion intercept: $c' = a' \cdot \tan\phi'$ (Senneset et al. 1989). Similarly, the porewater parameter B_q is determined as the slope of Δu vs. net cone resistance (Fig. 18b), giving $B_q = 0.75$ for the Sandpoint site. These values are entered into the solution chart in Figure 16, finding a representative $\phi' = 33°$ for the clayey silt. Finally, this value compares exceptionally well with extensive series of 30 laboratory CIUC triaxial tests conducted on undisturbed samples taken over a range of depths at the site (Figure 19).
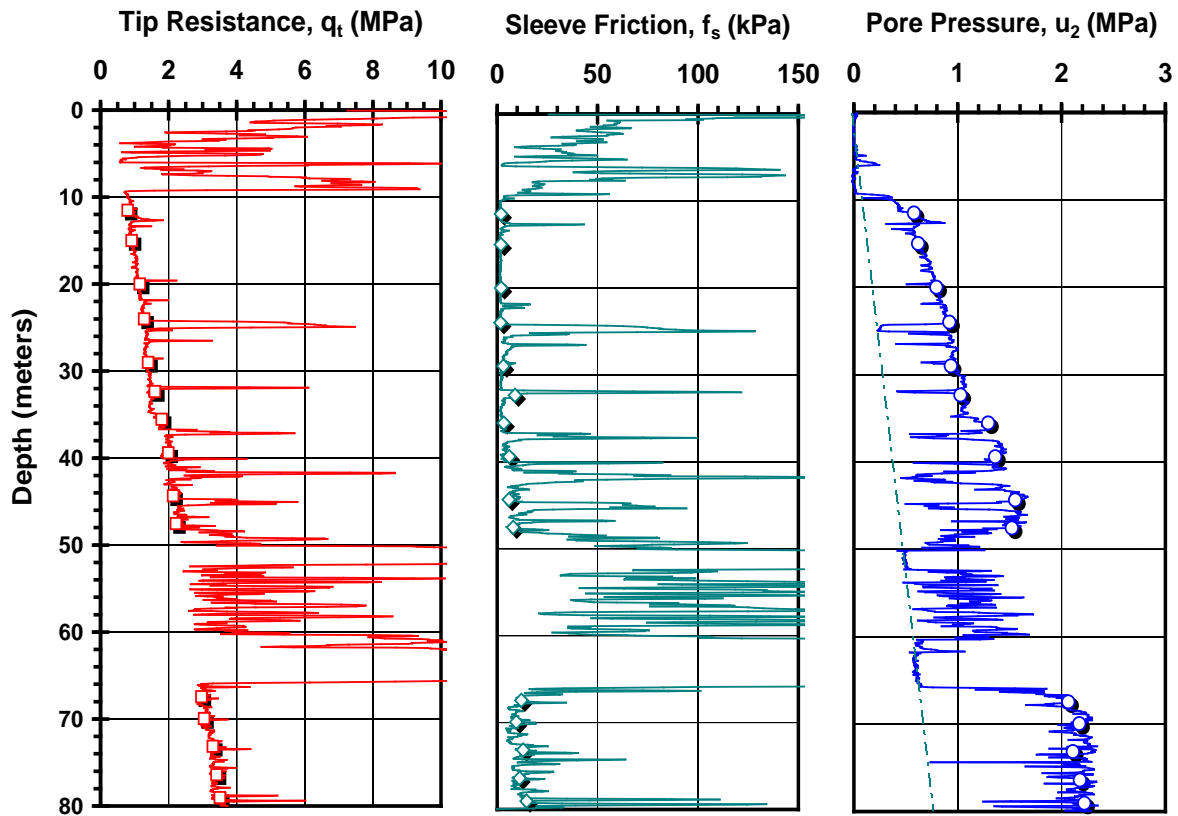
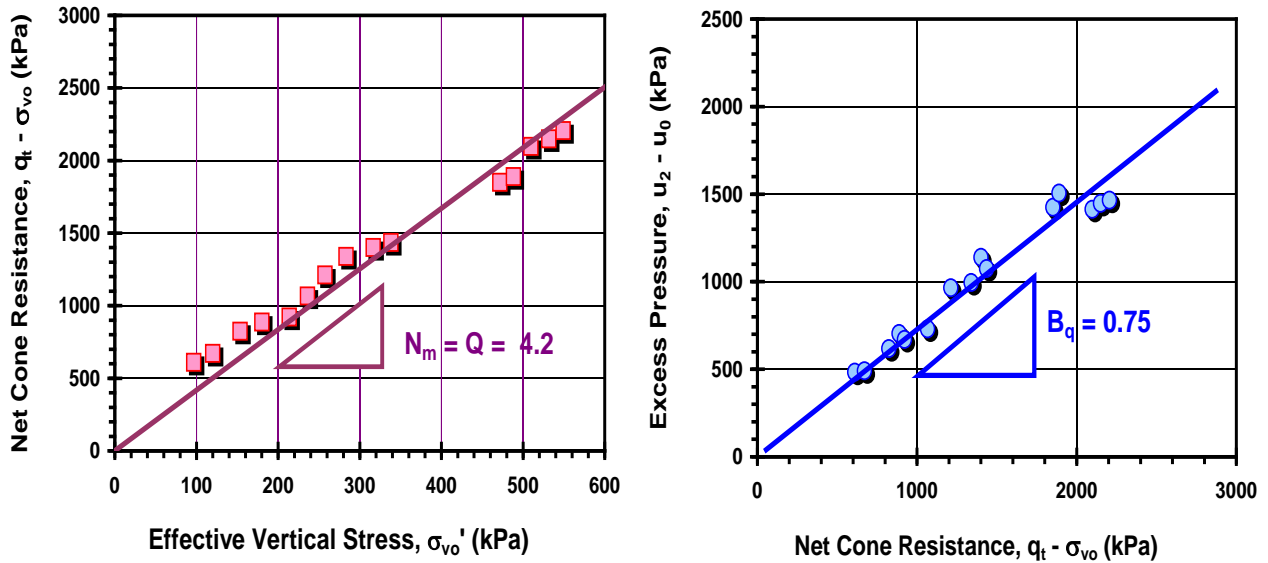Figure 17. Piezocone sounding in soft clayey silt at Sandpoint, Idaho (courtesy Dean Harris - CH₂M-Hill)

Figure 18. NTH post-processing of CPTu data at Sandpoint Idaho for determination of (a) cone resistance number, N_m (b) porewater pressure parameter, B_q.
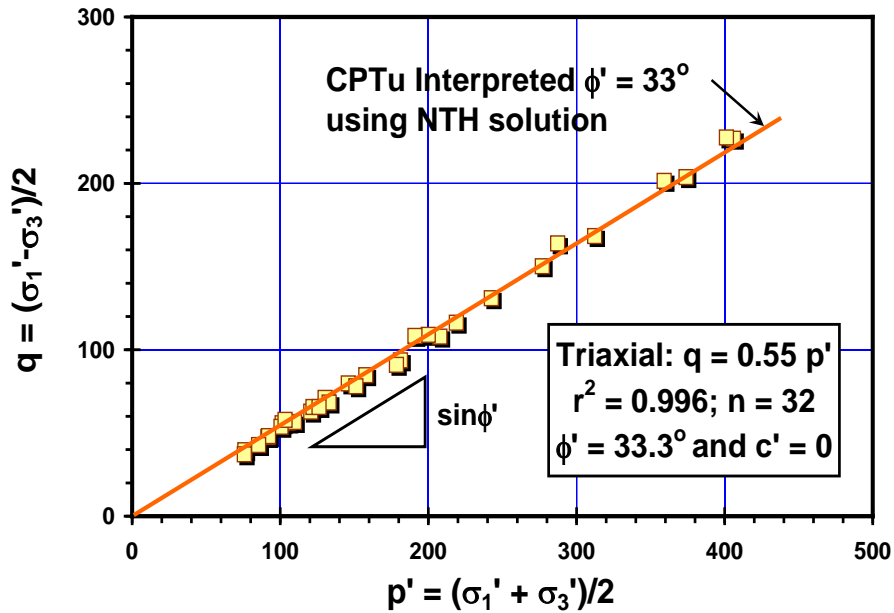
Figure 19. Summary of effective friction angles determined from CIUC triaxial shear tests and CPTu-NTH solution on soft clayey silt at Sandpoint, Idaho.

For cases involving soft to firm clays when c' = 0 (thus $N_m = Q_{t1}$) and assuming β = 0, an approximate algorithm for the NTH solution has been devised (Mayne 2005) to allow a line-by-line analysis, easily handled by computer software or spreadsheets:

$$\phi' \text{ (degrees)} = 29.5° \, B_q^{0.121} \, [0.256 + 0.336 \, B_q + \log Q_{t1}] \tag{21}$$

which is applicable for the following ranges of parameters: $20° \leq \phi' \leq 45°$ and $0.1 \leq B_q \leq 1.0$. At this time, the use of (21) should be restricted to clays, silts, and mixed soils with low OCRs < 2 until full calibration of this approach has been verified.

6 STRESS HISTORY

6.1 *Geostatic stress state*

The stress history of clays is conventionally determined using one-dimensional consolidation tests on undisturbed soil samples to assess the effective yield stress (σ_y'), more commonly termed the preconsolidation stress (σ_p'). For silts and sands, this is more difficult as samples are difficult, expensive, and/or impossible to procure. Thus, stress history in these types of geomaterials generally must be evaluated by other means such as geologic evidence, captured embedded clay layers, groundwater, and ageing.

The normalized and dimensionless form for stress history is the yield stress ratio (YSR = σ_y'/σ_{vo}'), and in terms of its most common occurrence, the mechanical removal of overburden stresses due to erosion, glaciation, and excavation results in the overconsolidation ratio (OCR = σ_p'/σ_{vo}').

An alternate stress history parameter is the overconsolidation difference (OCD = $\sigma_p' - \sigma_{vo}'$) which is convenient for mechanically-preconsolidated deposits because the OCD value is constant at all elevations in the formation. This is in contrast to OCR that decreases with depth, or preconsolidation stress (σ_p') which increases with depth (Locat et al. 2003). Both σ_p' and OCR can be calculated directly from
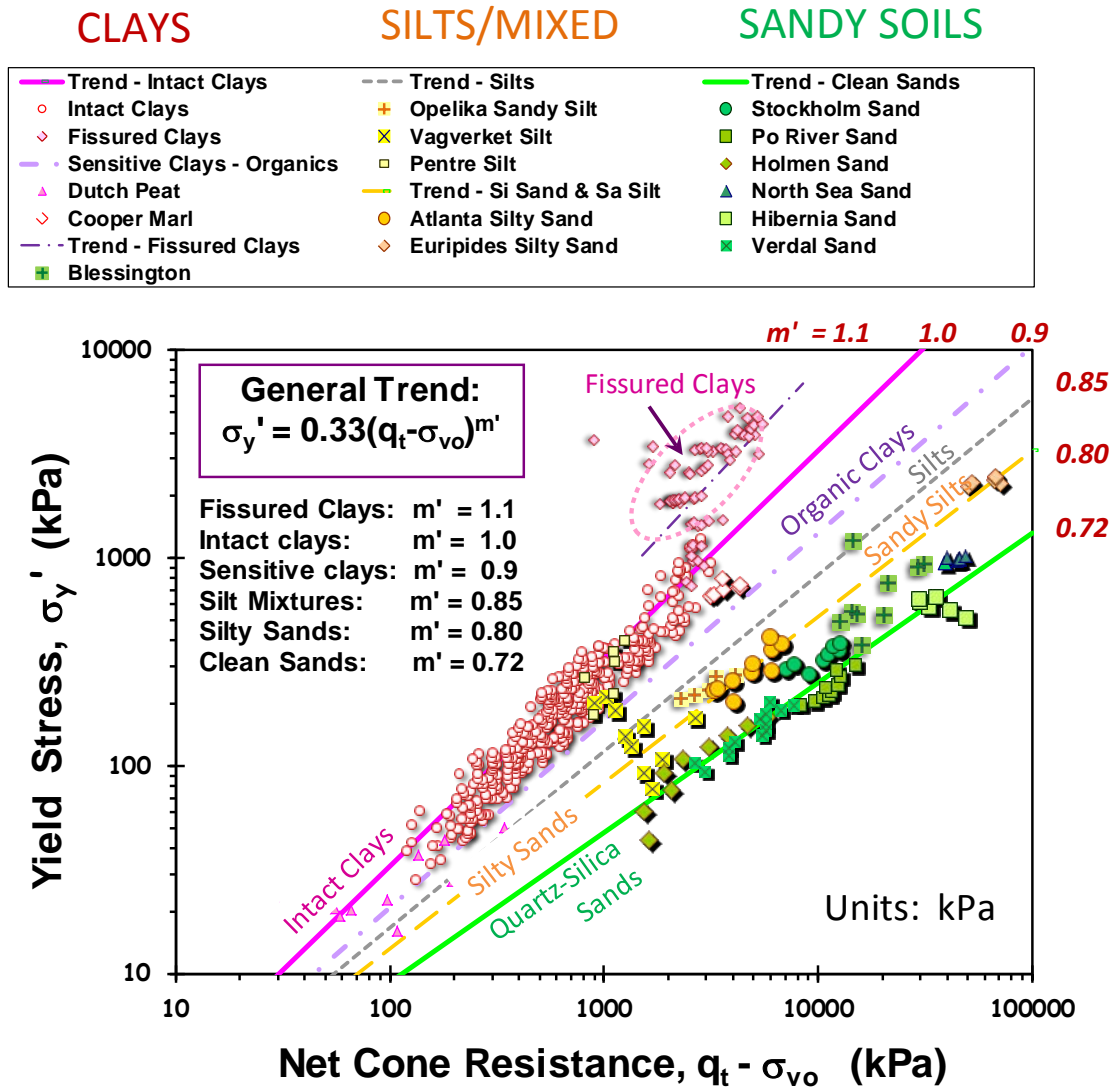
Figure 20. Yield stress vs. net cone resistance trend for clays, silts, sands, and mixed soil types (modified after Mayne et al. 2009)

the OCD and σ_{vo}' using: (a) $\sigma_p' = (OCD + \sigma_{vo}')$; (b) $OCR = (OCD/\sigma_{vo}' + 1)$. In the case of soils with quasi-preconsolidation caused by repeated wetting-drying, ageing, groundwater, cementation, and freeze-thaw cycles, the OCD can only provide an approximate representation.

6.2 *Interpretation of yield stress from CPT*

A unified approach to the evaluation of effective yield stress in soils has been developed showing that the net cone tip resistance can provide a quick first-order estimate of yield stress (Mayne et al. 2009). The approach is presented in Figure 20 and is expressed by a power law:

$$\sigma_p' = 0.33 \cdot (q_t - \sigma_{vo})^{m'} (\sigma_{atm}/100)^{1-m'} \qquad (22)$$

where the exponent *m'* decreases with mean grain size (Mayne 2013). Based on available data, the parameter m' ≈ 0.72 in clean quartz to silica sands, 0.8 in silty sands, 0.85 in silts, 0.90 in organic and sensitive fine-grained geomaterials, and m' = 1.0 in intact clays of low sensitivity. For fissured clays, a val-

ue of m' ≈1.1+ may be applicable. For intact clays, it can be viable to use the excess porewater pressures (Δu_2) and the effective cone tip resistance (q_t-u_2) to profile OCRs with depth (Mayne 2005).

The CPT material index I_c appears to be a means to directly assess the exponent parameter m' for general profiling of σ_p' in homogeneous and/or heterogeneous ground, as well as mixed soils, layered deposits, and/or stratified formations. Figure 21 shows a plot of exponent m' with CPT index I_c for young and uncemented soils (primarily quartz-silica "hourglass" sands to non-structured "vanilla" clays). The exponent m' can be expressed:

$$m' = 1 - \frac{0.28}{1 + (I_c/2.65)^{25}}$$

(23)

Caution is warranted towards application of these relationships in micaceous, glauconitic, and cemented as well as uncemented carbonate sands, as verification has not been made at this time.
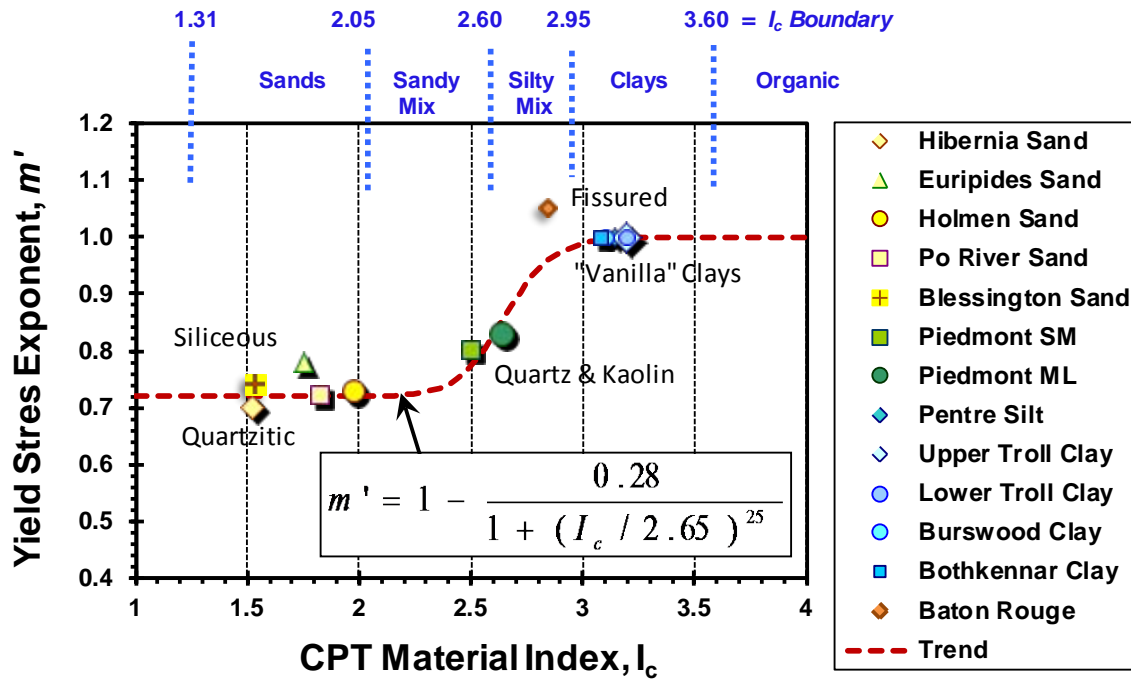

Figure 21. Observed trend for yield stress exponent m' with CPT material index, I_c.

6.3 Case study: Blessington sands

The unified expression for stress history can be applied to a new case study involving dense OC sands in Ireland reported by Tolooiyan & Gavin (2011) and Doherty et al. (2012). These glacially-derived dense fine sands have an in-situ relative density around 100% and mean particle size: $0.10 < D_{50}$ (mm) < 0.15 mm. Sand mineralogy is predominantly quartz with calcite, feldspar, mica, and kaolinite. Measured cone tip resistances from 4 CPT soundings are presented in Figure 22a, showing excellent repeatability.

Samples of the sand were procured by continuous sonic drilling for the laboratory, including triaxial compression testing for ϕ_p' evaluations and one-dimensional consolidation to define the yield stress (σ_y') per Casagrande method. Figure 22b indicates that eqn (17), as well as (18), provide quite reasonable profiles of friction angle. The interpreted profiles of OCR from the CPT using eqn (22) are shown in Figure 23 in comparison to the lab reference values, with excellent agreement noted for this site.
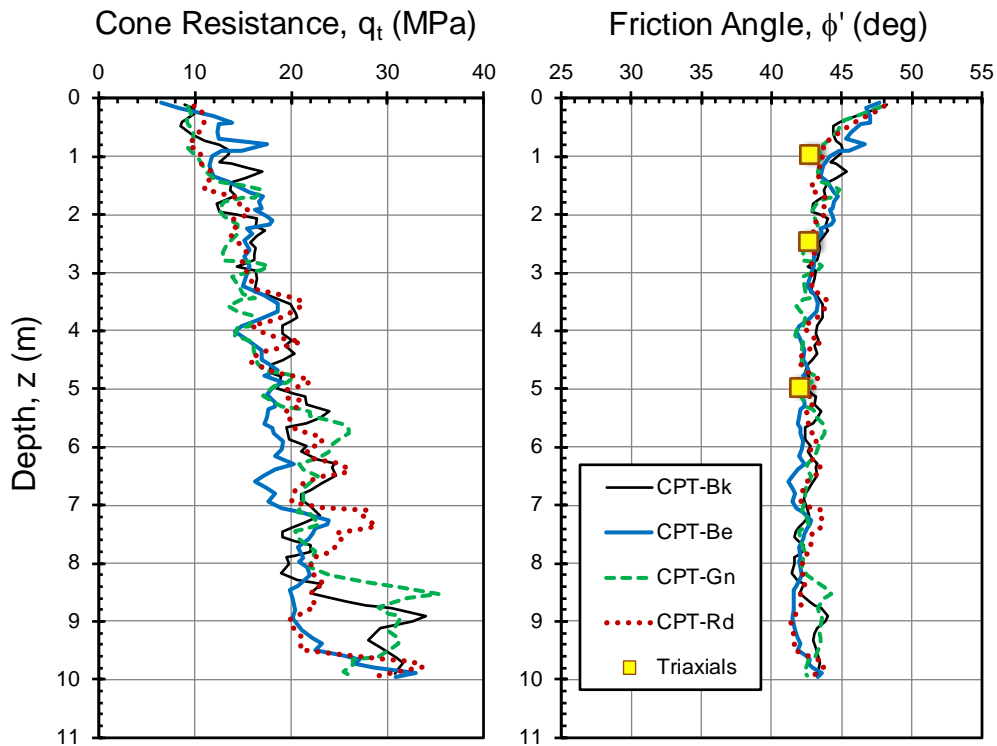
Figure 22. Profiles from Blessington sands: (a) CPT resistances; (b) interpreted peak friction angle. (data from Doherty et al. 2012)
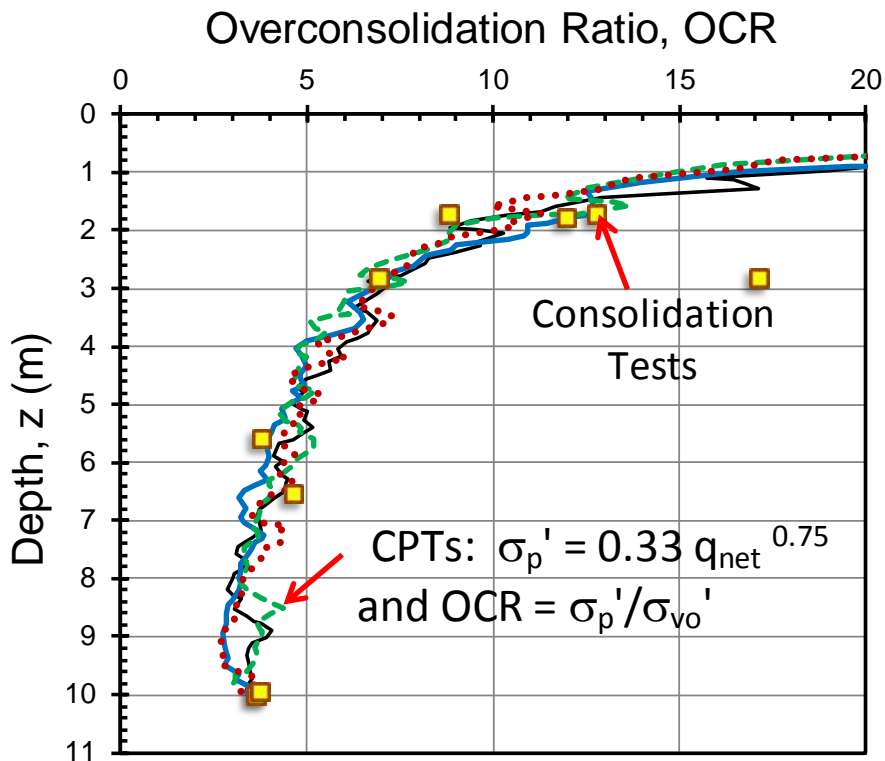

Figure 23. Profiles of OCR in Blessington sands using lab consolidometer results and CPT interpretation.

7 UNDRAINED SHEAR STRENGTH

In the general case of a Mohr-Coulomb strength criterion given by (14), the maximum shear stress is termed the shear strength and given by:

$$\tau_{max} = c' + (\sigma_{vo}' - \Delta u) \cdot \tan\phi' \tag{24}$$

For drained loading (often associated with clean sands), no excess porewater pressures are developed during shearing (i.e., $\Delta u = 0$). For clays, if the rate of loading is fast relative to the soil permeability, then there is no volume change ($\Delta V/V_0 = 0$) and the shear strength can represented by a total stress parameter: the undrained shear strength (designated $\tau_{max} = c_u = s_u$, or in the old vernacular, simple "c"). However, if the loading is slow enough, then drained conditions can prevail (especially over the thousands of years or even eons of time since deposition), and again: $\Delta u = 0$.

7.1 *Link to stress history*

For simple shearing of soils, the porewater pressure for the constant volume case (i.e. undrained loading) is given by:

$$\Delta u = (1 - \cos\phi'/2) \cdot OCR^\Lambda \cdot \sigma_{vo}' \tag{25}$$

For uncemented soils ($c' = 0$), equations (24) and (25) can be combined to provide the undrained shear strength in terms of effective friction angle and overconsolidation ratio (Mayne 2009):

$$s_u = (\sin\phi'/2) \cdot OCR^\Lambda \cdot \sigma_{vo}' \tag{26}$$

7.2 *Direct expressions*

While the above are rational outcomes from critical state soil mechanics, it is more common to find geotechnical practitioners directly evaluating s_u from net cone resistance (Lunne et al 1997):

$$s_u = (q_t - u_2)/N_{kt} \tag{27}$$

where the factor N_{kt} depends upon the mode of testing (e.g., vane, triaxial compression, simple shear, triaxial extension). In many cases, the simple shear mode is often close to the average of TC, DSS, and TE, thus a value $N_{kt} = 13.6 \pm 1.9$ may be appropriate for many situations in soft clays (Low et al. 2010). In addition to mode, the value of N_{kt} factor may depend on plasticity characteristics and stress history (Karlsrud et al. 2005).

In addition to the cone tip resistance, the measured excess porewater pressure may be used to profile the peak undrained shear strength:

$$s_u = (u_2 - u_0)/N_{\Delta u} \tag{28}$$

where the factor $N_{\Delta u} = 6.8 \pm 2.2$ may similarly be used for soft clays (Low et al. 2010).

Additionally, the effective cone resistance has been useful in evaluating the strength (Mayne & Chen 1993):

$$s_u = (q_t - u_2)/N_{ke} \tag{29}$$

where the factor $2 < N_{ke} < 10$ that tends to increase as the value of the porewater parameter B_q decreases (Karslrud et al. 2005).

Perhaps little known is a relationship that was developed between undrained shear strength (s_u in kPa) and shear wave velocity (V_s in m/s) for intact clays that is presented in Figure 24 and expressed as (Levesques et al. 2007):

$$s_u = (V_s/7.93)^{1.59} \tag{30}$$

Finally, the remolded shear strength may be assessed from the sleeve friction (Lunne et al. 1997):

$$s_{u(remolded)} \approx f_s \tag{31}$$

Therefore, all four readings from a seismic piezocone sounding can be applied towards an assessment of the undrained shear strength characteristics of a particular clay deposit.
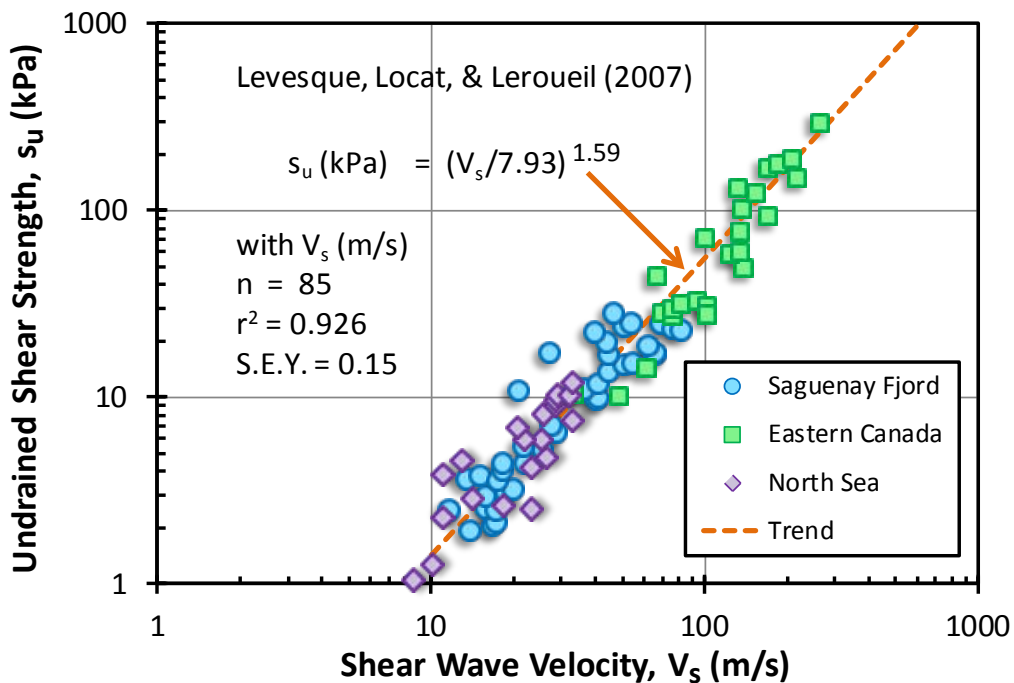
Figure 24. Relationship between undrained shear strength (s_u) and shear wave velocity for intact clays (modified after Levesques et al. 2007)

8 STIFFNESS

Soil stiffness can be represented by elastic parameters, including Young's modulus (E) or shear modulus (G) that are interrelated by:

$$E = 2G(1+\nu) \tag{32}$$

where ν = Poisson's ratio. The corresponding values of Poisson's ratio are often taken at the two general conditions: (a) constant volume (undrained), where $\nu_u = 0.5$; and (b) no excess porewater pressure (drained case), where $\nu' = 0.2$.

8.1 *Initial fundamental stiffness*

The stiffness of soils is highly nonlinear and begins with the small-strain shear modulus that is determined by the shear wave velocity:

$$G_{max} \; = \; G_0 \; = \; \rho_t \cdot V_s^2 \qquad\qquad (33)$$

where $\rho_t = \gamma_t/g_a$ = soil mass density, γ_t = total unit weight, and $g_a = 9.8$ m/s^2 = gravitational constant.

8.2 *Modulus reduction schemes*

The small-strain shear modulus (G_{max}) must be reduced to a secant or tangent value of shear modulus (G) that corresponds to the appropriate level of stress or relevant strain, depending upon the problem at hand. A number of different schemes for representing the modulus reduction curves (G/G_{max}) are available, as reviewed elsewhere (e.g., Tatsuoka & Shibuya 1992; Mayne 2005; Vardanega & Bolton 2013). These curves can be expressed either as functions of shear strain (γ_s) or mobilized stress level (Q/Q_{max}), where the latter can be considered as the reciprocal of the factor of safety (FS). In that regard, a first order estimate for the secant modulus reduction can be taken as:

$$(G/G_{max}) \; = \; 1 \; - \; (1/FS)^g \qquad\qquad (34)$$

where the exponent parameter *g* depends on the specific soil characteristics. Generally, 0.1 (soft response) $< g < 1.0$ (stiff response), with an assumed value $g \approx 0.3$ taken as a reasonable guestimate for uncemented and nonstructured geomaterials. Additional details on the application of (34) to providing approximate modulus evaluations from the initial fundamental stiffness G_{max} are given elsewhere (Fahey 1998, Mayne 2007).

8.3 *Direct modulus relationships from CPT*

Many attempts have been made to relate an elastic soil modulus to the measured cone tip resistance, often adopting either a linear expression ($E = \alpha_1 \cdot q_t + a_0$) or best-fit line ($E = a_2 \cdot q_t$) in the fitting arrangement. This can only be successful for a particular level of strain or specified FS, however, because soil stiffness is nonlinear throughout its regime.

A review of full-scale footing load tests from 32 foundations on 13 different sand formations (Uzielli & Mayne 2013) permits an evaluation of back calculated average Young's moduli in terms of a pseudo-strain (s/B), as shown in Figure 25. In this database, all footings have a realistic size with $0.5 < B < 6$ m so that issues with scale effects are not important. The moduli are normalized to a representative cone tip resistance taken as the average value over a depth equal to 1.5B beneath the foundation bearing elevation. The sands were primarily quartz to silica type sands with additional details given by Mayne & Illingworth (2010). These results have also been supplemented with data from 8 footings (4 reinforced concrete bases and 4 steel plates) situated on carbonate dune sands at Ledge Point (Lehane 2011). Statistical analyses on the separate sets of footings on silica-quartz sands (n = 262; $r^2 = 0.845$) and carbonate sand (n = 356; $r^2 = 0.790$) showed the moduli ratio (E'/q_t) from the latter set only 10% lower than the former set. Taken all together, the approximate trend for normalized soil modulus for square (or equivalent square) footings can be estimated as:

$$E'/q_t \; = \; 0.5 \, (s/B)^{-0.5} \qquad\qquad (35)$$

Measured cone tip resistances in the database ranged from 1.5 to 11 MPa. The observed ratio of modulus to tip resistance in Figure 25 compares similarly with traditional values of $\alpha = E'/q_t$. That is, the traditional range of $2 < \alpha < 10$ implies a range of displacements: $0.002 < s/B < 0.06$. For illustration, using the common tolerance criteria of s < 25mm for settlement at s/B = 0.01, a footing with B > 2.5m would correspond to $E'/q_t \sim 5$.

9 CONCLUSIONS AND FINAL REMARKS

For geotechnical site characterization, multiple readings from seismic piezocone tests (SCPTu) are most valuable in the assessment of soil engineering parameters. Generally, the SCPTu provides four profiles with depth: q_t, f_s, u_2, and V_s, with options to add time rate of porewater dissipation (t_{50}), if needed. In some cases, double or triple determinations occur because each of the separate recordings affords an opportunity to evaluate a chosen geoparameter. Redundancy can be good in helping to hone in on a probable value or range of values, if separate evaluations tend to show convergence. On the other hand, discrepancies and conflicts in the various interpretations from the different readings should be considered a warning signal or "red flag". In such cases, the geotechnical practitioner might wish to request additional laboratory and/or other in-situ testing to help resolve these difficulties and explain the contrasts.

ACKNOWLEDGMENTS
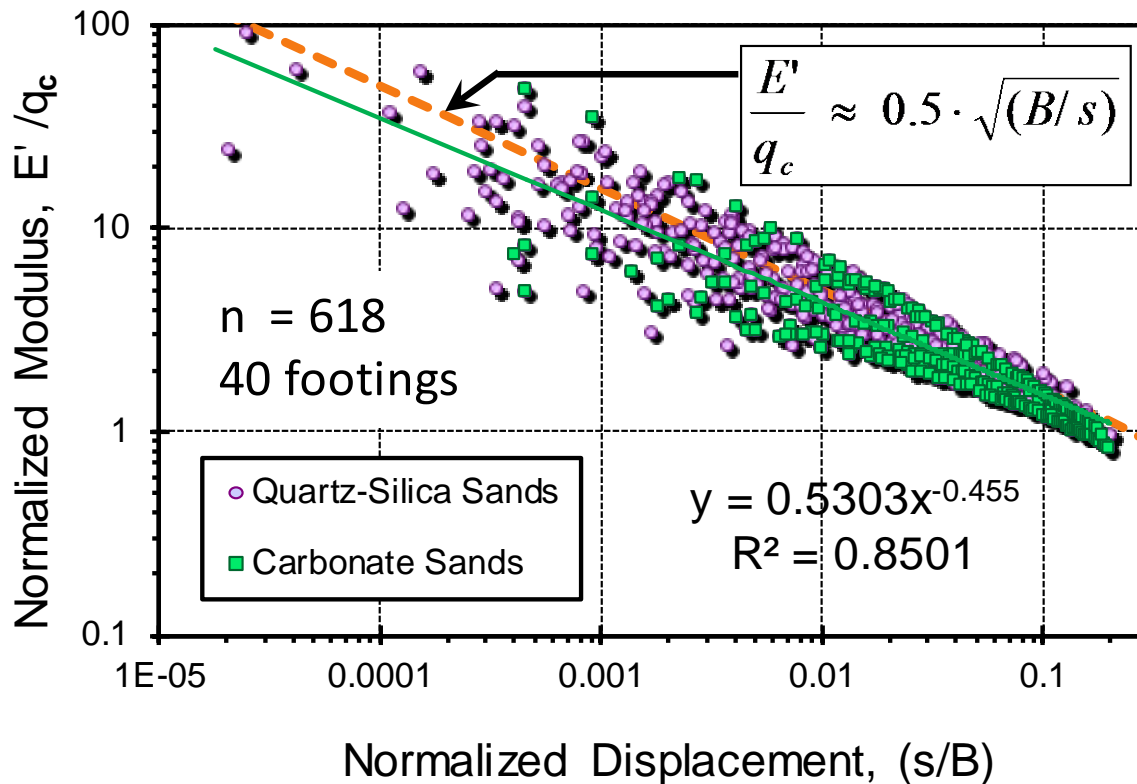
Figure 25. Backfigured modulus ratio versus normalized displacement (s/B) for 40 footings on 14 sands.

REFERENCES

Bolton, M.D. 1986. The strength and dilatancy of sands. *Geotechnique* 36 (1): 65-78.

Campanella, R.G., Robertson, P.K. and Gillespie, D. 1986. Seismic cone penetration test. *Use of In-Situ Tests in Geotechnical Engineering* (GSP 6), ASCE, Reston, VA: 116-130.

Cho, G-C., Dodds, J., and Santamarina, J.C. 2006. Particle shape effects on packing density, stiffness, and strength: natural and crushed sands. *J. Geotechnical & Geoenvironmental Engrg* 132 (5): 591-602.

Doherty, P., Kirwan, L. Gavin, K., Igoe, D. et al. (2012). Soil properties at the UCD geotechnical research site at Blessington. *Proc. Bridge and Concrete Research in Ireland*. Trinity College Dublin: 499-509. www.bcri.ie

Eslami, A. and Fellenius, B. H. 1997. Pile capacity by direct CPT-CPTu methods applied to 102 case histories. *Canadian Geotechnical Journal* 34 (6), 880 – 898.

Fahey, M. 1998. Deformation and in-situ stress measurements. *Geotechnical Site Characterization*, Vol. 1 (Proc. ISC-1, Atlanta), Balkema, Rotterdam: 49-68.

Fioravante, V., Jamiolkowski, M., Ghionna, V.N. Pedroni, S. 1998. Stiffness of carbonate Quiou sand. *Geotechnical Site Characterization*, Vol. 2 (Proc. ISC-1, Atlanta), Balkema, Rotterdam: 1039-1049.

Jamiolkowski, M., LoPresti, D.C.F., and Manassero, M. 2001. Evaluation of relative density and shear strength of sands from cone penetration test and flat dilatometer test. *Soil Behavior and Soft Ground Construction* (GSP 119), ASCE, Reston, VA: 201-238.

Jefferies, M. and Been, K. 2006. *Soil Liquefaction: A Critical State Approach*. Taylor & Francis Group, London: 408 p.

Karlsrud, K., Lunne, T., Kort, D.A. and Strandvik, S. 2005. CPTU correlations for clays. *Proc. 16th ICSMGE*, Vol. 2 (Osaka), Millpress, Rotterdam: 693-702.

Kim, T-H., Nam, J-M., Ge, L. and Lee, K-I. 2008. Settlement characteristics of beach sands and its evaluation. *Marine Georesources and Geotechnology* 26, Taylor & Francis, London: 67-85.

Kirsch, K. and Kirsch, F. 2010. *Ground Improvement by Deep Vibratory Methods*. Spon Press, Taylor & Francis Group, New York: 198 p.

Kulhawy, F.H. and Mayne, P.W. 1990. *Estimating Soil Properties for Foundation Design*. EPRI Report EL-6800, Electric Power Research Institute, Palo Alto: 306 p. www.epri.com

Lee, M.J., Hong, S.J., Kim, J.J. and Lee, W. 2010. Cone tip resistance of highly compressible Jeju beach sand. *GeoFlorida 2010: Advances in Analysis, Modeling, and Design* (GSP 199), ASCE, Reston, VA: 990-997.

Lehane, B.M. 2011. Shallow foundation performance in a calcareous sand. *Frontiers in Offshore Geotechnics II* (Proc. ISFOG, Perth), Taylor & Francis Group, London: 427-432.

Levesques, C.L, Locat, J. and Leroueil, S. 2007. Characterization of postglacial sediments of the Saguenay Fjord, Quebec. *Characterization and Engineering Properties of Natural Soils*, Vol. 4, Taylor & Francis Group, London: 2645-2677.

Locat, J., Tanaka, H., Tan, T.S., Dasari, G.R., and Lee, H. 2003. Natural soils: geotechnical behavior and geological knowledge. *Characterization and Engineering Properties of Natural Soils*, Vol. 1, Swets and Zeitlinger, Lisse: 3-28.

Low, H.E., Lunne, T., Andersen, K.H., Sjursen, M.A., Li, X. and Randolph, M.F. 2010. Estimation of intact and remoulded undrained shear strengths from penetration tests in soft clays. *Geotechnique* 60 (11): 843-859.

Lunne, T., Robertson, P.K., and Powell, J.J.M. (1997). *Cone Penetration Testing in Geotechnical Practice*, Blackie Academic/London, Routledge, New York: 312 p.

McRostie, G.C. and Crawford, C.B. 2001. Canadian Geotechnical Research Site No. 1 at Gloucester. *Canadian Geotechnical Journal* 38 (5): 1134-1141.

Mayne, P.W. and Chen, B.S.Y. 1993. Effective stress method for piezocone evaluation of undrained shear strength, *Proc. 3rd Intl. Conference on Case Histories in Geotechnical Engineering* (ICCHGE), Vol. 2, St. Louis, pp. 1305-1312.

Mayne, P.W., Christopher, B., Berg, R., and DeJong, J. 2002. *Subsurface Investigations - Geotechnical Site Characterization*. Publication No. FHWA-NHI-01-031, National Highway Institute, Federal Highway Administration, Washington, DC: 301 pages.

Mayne, P.W. 2005. Keynote: Integrated ground behavior: in-situ and lab tests. *Deformation Characteristics of Geomaterials*, Vol. 2. (Proc. IS-Lyon), Taylor and Francis Group, London: 155-177.

Mayne, P.W. 2007a. NCHRP *Synthesis 368: Cone Penetration Test*. Transportation Research Board, National Academies Press, Washington DC: 118 p. www.trb.org

Mayne, P.W. 2007b. Invited Overview Paper: In-situ test calibrations for evaluating soil parameters, *Characterization & Engineering Properties of Natural Soils*, Vol. 3 (Proc. IS-Singapore), Taylor & Francis Group, London: 1602-1652.

Mayne, P.W. 2009. *Geoengineering Design Using the Cone Penetration Test*. 155 pages. Published by ConeTec Inc., 12140 Vulcan Way, Richmond, BC, V6V 1J8: Website: www.conetec.com

Mayne, P.W., Coop, M.R., Springman, S., Huang, A-B., and Zornberg, J. 2009. State-of-the-Art Paper (SOA-1): Geomaterial Behavior and Testing. *Proc. 17th Intl. Conf. Soil Mechanics & Geotechnical Engineering*, Vol. 4 (ICSMGE, Alexandria, Egypt), Millpress/IOS Press Rotterdam: 2777-2872.

Mayne, P.W. 2013. Evaluating yield stress of soils from laboratory consolidation and in-situ cone penetration tests. *Sound Geotechnical Research to Practice* (Holtz Volume) GSP 230, ASCE, Reston/VA: 406-420.

Mayne, P.W. and Illingworth, F. 2010. Direct CPT method for footings on sand using a database approach. *Proc. 2nd Intl. Symposium on Cone Penetration Testing,* Vol. 3 (CPT'10), Omnipress: 315-322. www.cpt10.com

Mayne, P.W. and Peuchen, J. 2012. Unit weight trends with cone resistance in soft to firm clays. *Geotechnical and Geophysical Site Characterization 4,* Vol. 1 (Proc. ISC-4, Pernambuco), CRC Press, London: 903-910.

Miller, B. 2012. Personal communication: CPT data from the Canadian Research Test Site No. 1, South Gloucester, Ontario by ConeTec, Berlin, NJ.

Morioka, B.T. & Nicholson, P.G. 2000. Evaluation of liquefaction of calcareous sand, *Proc.10th Intl. Symposium on Offshore and Polar Engineering*, Vol. II, Seattle: p. 494-500.

Nutt, N.R.F. & Houlsby, G.T. 1991. Cone pressuremeter in Carbonate (Dogs Bay) sand. *Calibration Chamber Testing*, Elsevier, New York: 265-276.

Parkin, A.K. 1991. Chamber testing piles in calcareous sand & silt. *Calibration Chamber Testing* (ISOCCT, Potsdam), Elsevier, New York: 289-302.

Robertson, P. K. 1990. Soil classification using the cone penetration test. *Canadian Geotechnical Journal* 27 (1), 151 – 158.

Robertson, P.K. 2009. Interpretation of cone penetration tests – a unified approach. *Canadian Geotechnical Journal* 49 (11): 1337-1355.

Robertson, P.K. 2010. Estimating in-situ state parameter in sandy soils from the CPT. *Proc., 2nd Intl. Symposium on Cone Penetration Testing*, Vol. 3, (CPT '10, Huntington Beach), Omnipress: www.cpt10.com

Robertson, P.K. and Cabal, K.L. 2010. Estimating unit weight from CPT. *Proc., 2nd Intl. Symposium on Cone Penetration Testing*, Vol. 3, (CPT '10, Huntington Beach), Omnipress: www.cpt10.com

Robertson, P.K. 2012. The James K. Mitchell Lecture: Interpretation of in-situ tests - some insights. *Geotechnical and Geophysical Site Characterization 4*, Vol. 1 (Proc. ISC-4, Pernambuco), Taylor & Francis Group, London: 3 - 24.

Salgado, R., Mitchell, J.K., and Jamiolkowski, M. 1998. Calibration chamber size effects on penetration resistance in sands. *Journal of Geotechnical & Geoenvironmental Engineering* 124 (9): 878-888.

Sandven, R. and Watn, A. 1995. Theme lecture: interpretation of test results. Soil classification and parameter evaluation from piezocone tests. Results from Oslo airport. *Proc. Intl. Symposium on Cone Penetration Testing*, Vol. 3, Swedish Geotechnical Society Report SGF 3:95, Linköping: 35-55.

Schnaid, F. 2009. *In-Situ Testing in Geomechanics: The Main Tests*. Taylor & Francis Group, London: 330 p.

Schneider, J.A., Randolph, M.F., Mayne, P.W., and Ramsey, N.R. 2008. Analysis of factors influencing soil classification using normalized piezocone tip resistance and pore pressure parameters. *Journal of Geotechnical & GeoEnvironmental Engineering* 134 (11): 1569-1586.

Senneset, K., Sandven, R. and Janbu, N. 1989. Evaluation of soil parameters from piezocone tests. *Transportation Research Record 1235*, National Academies Press, Washington, DC: 24-37.

Skempton, A.W. 1986. Standard penetration test procedures and the effects in sands of overburden stress, relative density, particle size, ageing, and overconsolidation. *Geotechnique* 36 (3): 425-447.

Tatsuoka, F. and Shibuya, S. 1992. Deformation Characteristics of Soils and Rocks from Field and Laboratory Tests. *Report of the Institute of Industrial Science* Vol. 37, No. 1, University of Tokyo: 136p.

Tokimatsu, K., Suzuki, Y., Taya, Y. and Kubota, Y. 1995. Correlation of CPT data with static and dynamic properties of in-situ frozen sands. *Proc. CPT'95*, Vol. 2, Swedish Geotechnical Society: 323-328.

Tolooiyan, A. and Gavin, K. 2011. Modelling the cone penetration test in sand using cavity expansion and arbitrary Lagrangian Eulerian finite element methods. *Computers and Geotechnics* 38, Elsevier: 482-490.

Tumay, M., Abu-Farsakh, M., and Zhang, Z. 2008. From theory to implementation of a CPT-based probabilistic and fuzzy soil classification. *From Research to Practice in Geotechnical Engineering* (GSP 180), ASCE, Reston, VA: 259-276.

Uzielli, M., Mayne, P.W. and Cassidy, M.J. (2013). Probabilistic assessment of design strengths for sands from in-situ testing data. *Modern Geotechnical Design Codes of Practice*, Advances in Soil Mechanics & Geotechnical Engineering (series), Vol. 1, IOS-Millpress, Amsterdam: 214-227.

Vardanega, P. J. and Bolton, M. D. 2013. "Stiffness of clays and silts: normalizing shear modulus and shear strain." *Journal of Geotechnical and Geoenvironmental Engineering* 139 (9): 1575 – 1589.

Wehr, W.J. 2005. Influence of the carbonate content of sand on vibrocompaction. *Proc. 6th International Conference on Ground Improvement Techniques*, Coimbra, Portugal: 525-632.

Yu, H-S. and Mitchell, J.K. (1998). Analysis of cone resistance: review of methods. *Journal of Geotechnical & Geoenvironmental Engineering* 124 (2): 140-149.